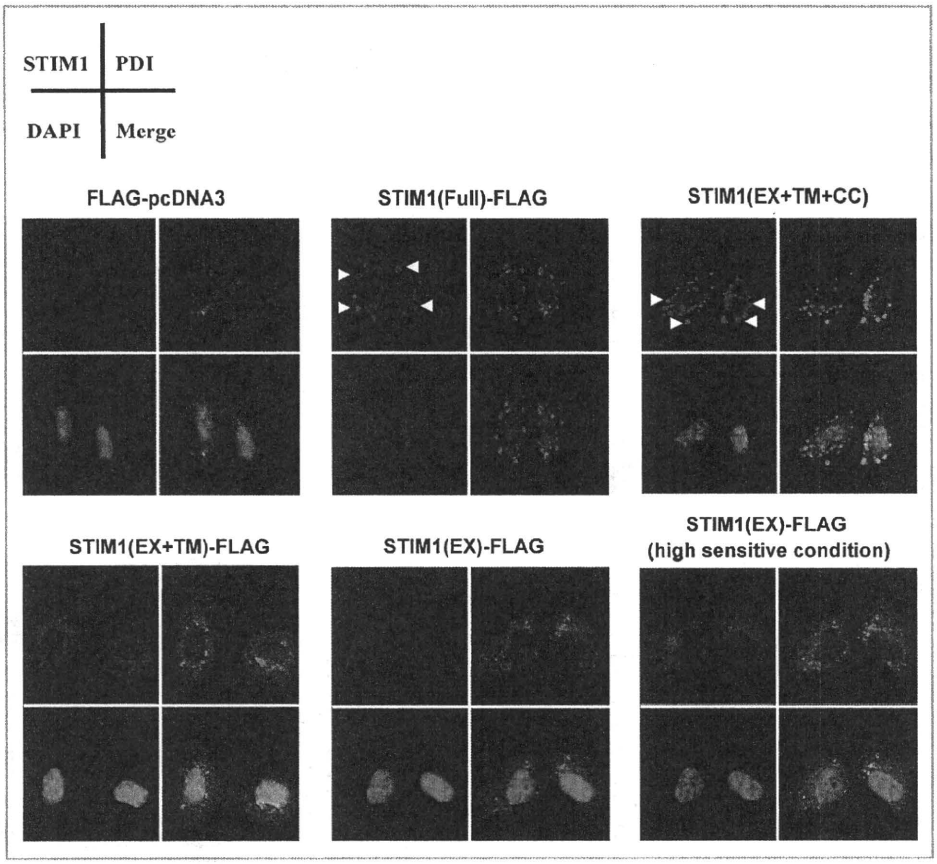

Fig. 2. Overexpression of STIM1 induces shape changes in ER. HeLa cells were transfected with the indicated STIM1 mutant expression plasmids. After 24 h, each transfectants was fixed and reacted with mouse anti-FLAG M2 and rabbit anti-PDI antibodies, and visualized with Alexa Fluor® 568 goat anti-mouse IgG and Alexa Fluor® 488 goat anti-rabbit IgG. PDI was used for the indication of ER. The same slide also was stained with DAPI for the nuclei staining. All images were taken with confocal microscopy. White arrow heads indicate the distended form of ER. Similar results were obtained in six independent experiments.

importin, all of which are involved in protein trafficking [Siomi et al., 1997; Hutten and Kehlenbach, 2007; Okada et al., 2008], were frequently scored in the approximately 100–110 kDa band (band 1). Because all bands included keratin protein, it seemed to be non-specific. Calnexin, exportin1, transportin1, or importin was never scored in the equivalent negative control samples. Therefore, we identified calnexin, exportin1, transportin1, and importin as possible STIM1-associated proteins in cells.

CALNEXIN, EXPORTIN1, AND TRANSPORTIN1 BIND TO BOTH STIM1 AND STIM2

The binding specificity between STIM1 and calnexin was confirmed with the co-immunoprecipitation studies. Using the cell lysates from 293T as well as HeLa cells transfected with STIM1(Full) or FLAG-pcDNA3 plasmid, immunoprecipitation with anti-FLAG antibody was performed. The precipitates for STIM1 contained calnexin, as expected (Fig. 6A and data not shown). Similarly, the precipitates contained exportin1 and transportin1. However, it was not clear whether the precipitates contained importin (data not shown). The specific association of STIM1 with calnexin, exportin1, and transportin1 were also observed even when we used HeLa cells (data not shown). To assess whether this association is physiological, cell lysates from HeLa were immunoprecipitated with anti-STIM1 antibody and were subjected to Western-blot using anti-calnexin, anti-exportin1, and anti-transportin1. As shown in Figure 6B, the precipitates for endogenous STIM1 in HeLa cells contained calnexin, exportin1 and transportin1, indicating that STIM1 physiologically interacts with these proteins. However, the binding of STIM1 to these molecules is unlikely to be depending on Ca^{2+} because it was observed even in the presence of EDTA (data not shown). We analyzed whether these molecules can bind to STIM2, which has a high homology with STIM1. After transient transfection of plasmid for FLAG-tagged STIM2 into 293T cells, the cell lysate was immunoprecipitated with anti-FLAG antibody and subjected to Western-blotting analysis. The immunoprecipitates for STIM2 also contained calnexin, exportin1, and transportin1, similarly to those

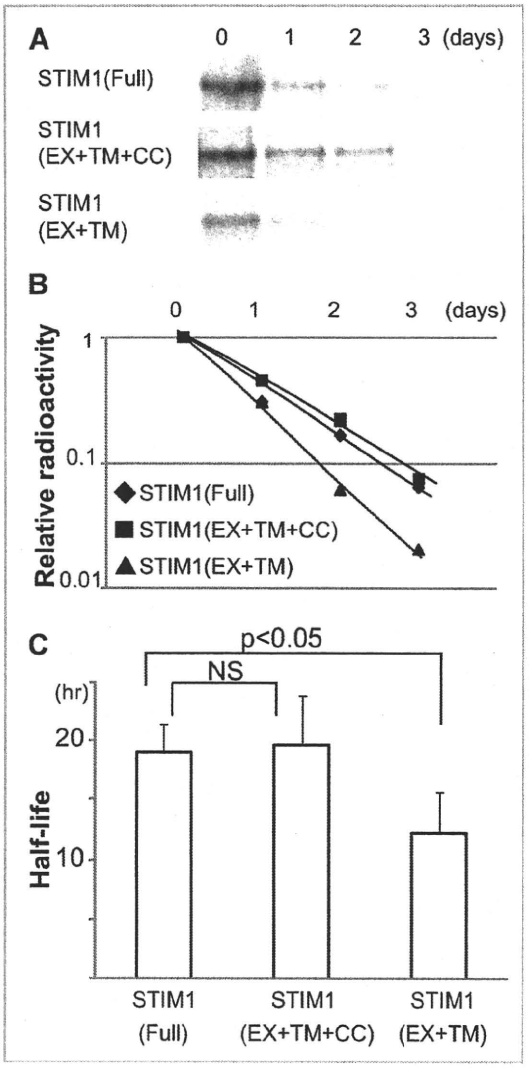

Fig. 3. The coiled-coil domains of STIM1 contribute its protein stability. A: After transient transfection of the indicated plasmids to HeLa cells, the cells were pulse-labeled with ^{35}S-methionine for 1 h and then chased for the indicated periods. The labeled cells were lysed and subjected to the precipitation with ANTI-FLAG® M2-Agarose Affinity Gel. The precipitates were separated on SDS-PAGE gels, and the gels were dried, and autoradiographed. B: The radioactivity of specific bands corresponding to each STIM1 mutant was measured with ImageGauge 4.22 software. Means of three independent experiments are shown. The plot uses logarithmic scaling on the vertical line. C: Data are shown as mean ± SD of half life of STIM1 mutant proteins in three independent experiments. NS, not significant differences.

for STIM1 (Fig. 6A). Therefore, both STIM1 and STIM2 can associate with calnexin, exportin1, and transportin1.

CALNEXIN BINDS TO STIM1 INDEPENDENTLY OF GLYCOSYLATION STATE

Calnexin is a transmembrane protein localized in ER. Calreticulin, an ER-resident soluble protein, has high sequence homology with

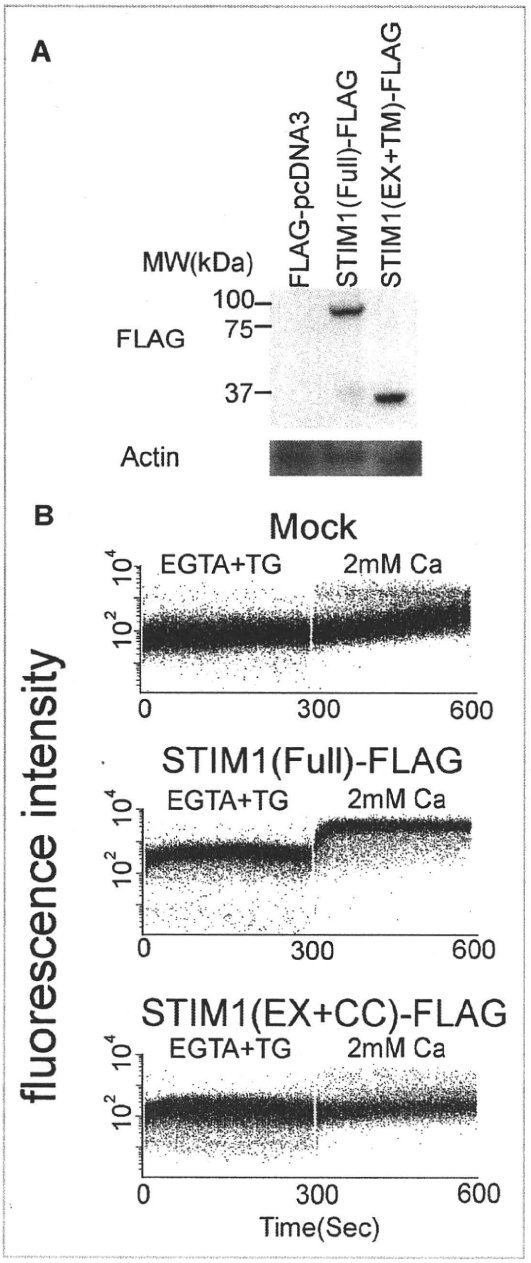

Fig. 4. The cytoplasmic region of STIM1 is essential for activating SOCE. A: Plasmids for FLAG-pCDNA3, FLAG-tagged STIM1(Full), and STIM1(EX + TM) were stably transduced in STIM1-deficient DT40 B cells, and each expressed protein was detected with Western-blot using anti-FLAG antibody. Actin was detected as a loading control. B: Intracellular Ca^{2+} mobilization was monitored by Fluo4 imaging in DT40 cells expressing STIM1(Full) and STIM1(EX + TM). The transfected DT40 cells were treated with 10 μM thapsigargin(TG) in the absence of extracellular Ca^{2+} (0.5 mM EGTA) to deplete Ca^{2+} stores. Ca^{2+} influx was monitored after adding 2 mM Ca^{2+} in each DT40 cell clone. Data are representative of three independent experiments.

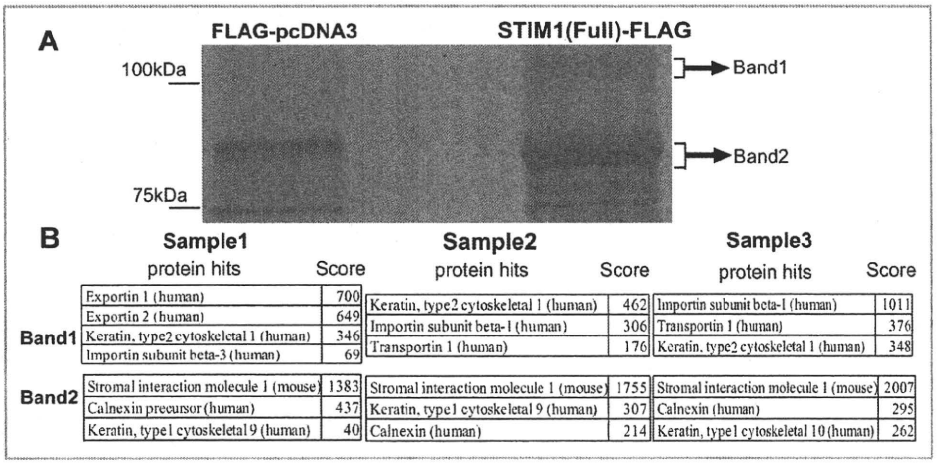

B

	Sample1 protein hits	Score	Sample2 protein hits	Score	Sample3 protein hits	Score
Band1	Exportin 1 (human)	700	Keratin, type2 cytoskeletal 1 (human)	462	Importin subunit beta-1 (human)	1011
	Exportin 2 (human)	649	Importin subunit beta-1 (human)	306	Transportin 1 (human)	376
	Keratin, type2 cytoskeletal 1 (human)	346	Transportin 1 (human)	176	Keratin, type2 cytoskeletal 1 (human)	348
	Importin subunit beta-3 (human)	69				
Band2	Stromal interaction molecule 1 (mouse)	1383	Stromal interaction molecule 1 (mouse)	1755	Stromal interaction molecule 1 (mouse)	2007
	Calnexin precursor (human)	437	Keratin, type1 cytoskeletal 9 (human)	307	Calnexin (human)	295
	Keratin, type1 cytoskeletal 9 (human)	40	Calnexin (human)	214	Keratin, type1 cytoskeletal 10 (human)	262

Fig. 5. Identification of STIM1 associated molecules. A: 293T cells were transfected with STIM1(Full)-FLAG or FLAG-pcDNA3 (control). After 3 days, each transfectant (approximately 2×10^8 cells) was lysed and precipitated with ANTI-FLAG® M2-Agarose Affinity Gel. The precipitates were electrophoresed on SDS-PAGE gels, and the gels were stained with silver staining. The specific bands in the lane for STIM1(Full)-FLAG-transfected samples were indicated as band 1 and 2. B: The specific bands were excised from the gel, digested with TrypsinGold, and subjected to mass spectrometry. The analyzed data of three independent experiments for band 1 and 2 are shown with score.

calnexin [Ni and Lee, 2007; Caramelo et al., 2008]. Both proteins are sugar-binding chaperones, which recognize $Glc_1Man_9GlcNAc_2$ structure during a transient oligosaccharide-processing of newly synthesized glycoproteins. Thus, we investigated whether calreticulin, like calnexin, can bind to STIM1. In both HeLa and 293T cells, the immunoprecipitates for STIM1 contained calnexin, but not calreticulin (Fig. 6C), suggesting that the binding between STIM1 and calnexin was specific and that the binding might not be depending on glycosylation state. Thus, we analyzed the binding between STIM1 and calnexin in HeLa cells treated with tunicamycin, a glycosidase inhibitor. As shown in Figure 7A, tunicamycin-treatment of HeLa cells did not cancel the recognition of STIM1 by calnexin. In addition, calnexin could still recognize a STIM1(del-Gly) mutant whose two Asn-linked glycosylation sites were destroyed (Fig. 7B). Therefore, glycosylation on STIM1 is not required for the association between STIM1 and calnexin.

DISCUSSION

Despite a great number of recent studies showing the molecular organization of STIMs, which link Ca^{2+}-store depletion, several aspects remain to be resolved. We are now uncertain how STIM1 retains in ER, how the protein content of STIM1 is regulated, how STIM1 travels in parallel with Ca^{2+} concentration, and so on. In the present study, experiments using the deletion mutants of STIM1 revealed that the coiled-coil domains are critical for its ER-retention and protein stability, and that the cytoplasmic region is essential for activating SOCE. In addition, we identified calnexin, exportin1, and transportin1 as new STIM-associated proteins. These findings could help us understand functional mechanisms and protein characters of STIMs.

Once the nascent polypeptide chains emerge into an ER lumen, they receive a series of modifications, such as signal peptide cleavage, glycosylation, protein folding, and disulfide-bond formation [Bauer et al., 2008; Honnappa et al., 2009]. In ER, newly synthesized proteins are protected by chaperones, which are involved in the quality control of newly synthesized proteins. Only correctly folded proteins can traverse the secretory pathway leading to Golgi apparatus while misfolded and/or abnormal proteins can not exit from ER and are degraded. With regard to the trafficking of proteins between ER and Golgi, there are two ways of transports: the anterograde ER-to-Golgi transport and the retrograde Golgi-to-ER transport [Hawes et al., 2008; Spang, 2009]. Thus, the balance between anterograde and retrograde transports determines the steady-state distribution of proteins. As widely accepted, STIM1 mainly localizes in ER. With a signal trap method, we first cloned STIM1 (we originally named SIM) as a protein which has a signal peptide at N-terminus [Oritani and Kincade, 1996]. We produced and screened fusion proteins composed of cDNA-derived protein (N-terminal portion), a HPC4-tag, and a tissue factor-transmembrane. In this case, our isolated STIM1 cDNA did not contain the cytoplasmic regions. That is likely to be a reason why we recognized STIM1 as a novel cell surface protein. In general, a large number of ER-resident proteins have ER-retention signals, such as KDEL (or similar sequences) or KKXX/KXKXX, at their C-terminal position [Munro and Pelham, 1987; Nilsson et al., 1989; Jackson et al., 1990]. Of importance, STIM1 sequence does not have a possible ER-retention signal while STIM2 sequence does. Our present data strongly indicated that the coiled-coil domains were essential for the ER-retention of STIM1. It is noteworthy that some ER-resident proteins do not have ER-retention signals mentioned above. For example, an ER-localized protein, Sec71p does not have a typical ER-retention motif, but contains a Rer1p-recognized region in its transmembrane domain [Sato et al., 1997]. In the case of STIM1, there might be a hidden ER-retention sequence in the cytoplasmic region corresponding to the coiled-coil domains, similarly to the

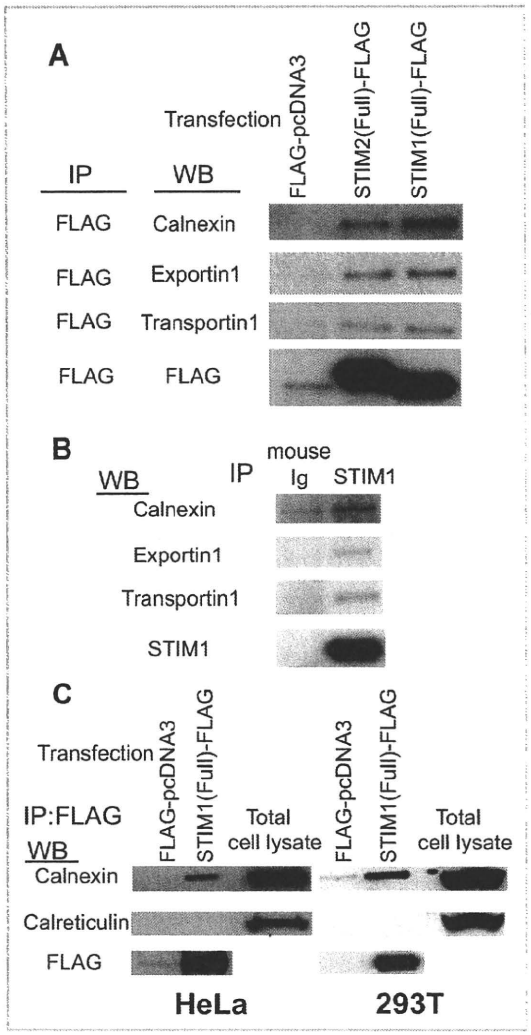

Fig. 6. Both STIM1 and STIM2 associate with calnexin, exportin1, and transportin1. A: After transient transfection of STIM1(Full)-FLAG or STIM2(-Full)-FLAG to 293T cells, each transfectant was lysed, precipitated with ANTI-FLAG® M2-Agarose Affinity Gel, and subjected to Western blot using specific antibodies against the indicated molecules. B: Cell lysates of HeLa cells were immunoprecipitated with anti-STIM1 antibody, and the precipitates were subjected to Western blot using specific antibodies against the indicated molecules. C: After transient transfection of STIM1(Full)-FLAG to 293T or HeLa cells, the transfectants were lysed and immunoprecipitated with ANTI-FLAG® M2-Agarose Affinity Gel, and subjected to Western-blotting analysis using specific antibodies against the indicated molecules. The cell lysates of 293T or HeLa cells were used as controls for positive staining. Similar results were obtained in three independent experiments.

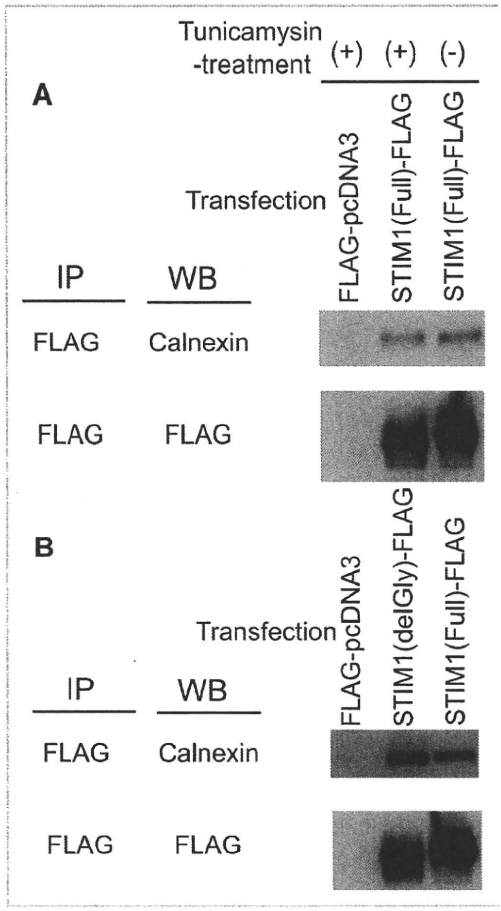

Fig. 7. Calnexin binds to STIM1 independently of glycosylation state. A: HeLa cells were transfected with STIM1(Full)-FLAG or FLAG-pcDNA3. After 12 h of cultures, the transfectants were treated with or without tunicamycin (10 μM) for 2 days. The treated cells were then lysed, precipitated with ANTI-FLAG® M2-Agarose Affinity Gel, and subjected to Western blot using anti-calnexin antibody. Similar results were obtained in three independent experiments. B: HeLa cells were transfected with STIM1(Full)-FLAG, STIM1(delGly)-FLAG or FLAG-pcDNA3. Each transfectant was lysed, precipitated with ANTI-FLAG® M2-Agarose Affinity Gel, and subjected to Western blot using anti-calnexin antibody. Similar results were obtained in three independent experiments.

case of Sec71p. Alternatively, some association molecules of the coiled-coil domains might provide ER-retention signals.

Although the distended ER might be an artifact by over-expression systems, it clearly means the capacity of the expressed proteins to be accumulated in ER. STIM1 mutants (Full and EX + TM + CC), which change the shape of ER to "the distended form," exhibited lower potential to be expressed on cell surface. In addition, both mutants had longer half-life of proteins than those without the distention of ER. Of importance, the coiled-coil domains of STIM1 are involved in both the ER-retention and the protein stability. It should be resolved how the coiled-coil domains of STIM1 exhibit these interesting roles in cells, and experiments are now in progress in this regard.

We identified exportin1, transportin1, and calnexin as novel STIM-associated proteins. Exportin1 and transportin1 belong to a family of nuclear transport receptors. These receptors recognize the nuclear localization or export signals on protein or RNA cargoes, and then transport the complexes across nuclear pores [Siomi et al., 1997; Hutten and Kehlenbach, 2007]. Of course, our data can not

completely exclude problems resulting from the nonspecific binding. However, the immunoprecipitates for STIM1 selectively contained the two kinds of the transport receptors repeatedly, suggesting that the binding of STIMs to exportin1 and transportin1 might play a physical role although STIM proteins mainly exist in ER. Together, these results might be indicating a more complex mode of interactions. With regard to calnexin, it is a type I ER membrane protein and functions as a carbohydrate-binding chaperone [Ni and Lee, 2007; Caramelo and Parodi, 2008]. Shortly after the addition of core oligosaccharide complex to nascent polypeptides, their terminal two glucose residues are removed by glycosidases I and II. This modification generates monoglycosylated oligosaccharides to which calnexin can bind. Further processing of oligosaccharides results in the release of newly synthesized glycoproteins from calnexin. Because STIM1 sequence has two putative Asn-linked glycosylation sites, STIM1, like other glycoproteins, might use calnexin for its quality control in ER. On the other hand, calnexin also has an ability to associate with several proteins independently of its glycosylation state. Calnexin variants carrying point mutations in the lectin site can not recognize oligosaccharides but retain the ability to bind to ERp57 [Leach and Williams, 2004]. Another example is the case of ER degradation enhancing α-mannosidase-like protein (EDEM). The transmembrane domain of calnexin is known to bind to EDEM [Oda et al., 2003]. As described here, the treatment of HeLa cells with a glycosidase-inhibitor could not prevent the interaction between STIM1 and calnexin. In addition, a STIM1 mutant whose Asn-glycosylation sites were destroyed could still bind to calnexin. These results seem to indicate that the binding between STIM1 and calnexin does not require glycosylation, similar to the case of ERp57 or EDEM. Thus, calnexin may function on STIM1 beyond a chaperone protein.

Targeting of the calnexin or its related molecule calreticulin gene in mice has brought severe consequences. Calreticulin-deficient mice are embryonic lethal via cardiac defects, and their phenotype was rescued by the overexpression of activated calcineurin, which is a Ca^{2+}/calmodulin-dependent protein phosphatase [Guo et al., 2002]. Calnexin-deficient mice are viable but show neurological abnormalities [Denzel et al., 2002]. In addition, its important binding partner ERp57 is known to associate with and influence the SERCA2b Ca^{2+} pump [Li and Camacho, 2004]. Thus, calnexin/calreticulin systems presumably play roles in multiple processes beyond their functions of protein folding. For example, there are possible influences in ER Ca^{2+} homeostasis as well as cell shape, adhesion, and motility. Because STIMs are important Ca^{2+} sensors in ER, the association between STIMs and calnexin might have physical roles in intracellular Ca^{2+} regulation.

To date, several STIM-associated molecules have been reported. Overexpressed STIM1 associates with microtubule cytoskeleton, especially with EB1 [Honnappa et al., 2009]. The involvement of microtubule cytoskeleton in STIM functions has also been indicated [Smyth et al., 2007]. However, these associations are limited to the restricted cell types, and can explain only a part of regulatory mechanisms for STIM functions and/or stability. In the present study, our immunoprecipitation combined with mass spectrometry analysis for STIM1-associated molecules identified calnexin, exportin1, and transportin1. Although we used digitonin as a detergent in this screening, other STIM1-interacting molecules may be identified by utilizing CHAPS as another weak detergent. The coiled-coil regions, which we here demonstrated as interesting domains, could be suitable as bait for the screening. We will continue additional rounds of screenings with minor modifications. Further information concerning regulatory mechanisms for STIM proteins will provide a model of Ca^{2+} control as well as a useful strategy to develop therapeutic drugs for intracellular Ca^{2+}-related diseases, including inflammation and allergy.

REFERENCES

Baba Y, Kurosaki T. 2009. Physiological function and molecular basis of STIM1-mediated calcium entry in immune cells. Immunol Rev 231:174–188.

Bauer MC, O'Connell D, Cahill DJ, Linse S. 2008. Calmodulin binding to the polybasic C-termini of STIM proteins involved in store-operated calcium entry. Biochemistry 47:6089–6091.

Berridge MJ, Lipp P, Bootman MD. 2000. The versatility and universality of calcium signaling. Nat Rev Mol Cell Biol 1:11–21.

Berridge MJ, Bootman MD, Roderick HL. 2003. Calcium signalling: Dynamics, homeostasis and remodeling. Nat Rev Mol Cell Biol 4:517–529.

Caramelo JJ, Parodi AJ. 2008. Getting in and out from calnexin/calreticulin cycles. J Biol Chem 283:10221–10225.

Denzel A, Molinari M, Trigueros C, Martin JE, Velmurgan S, Brown S, Stamp G, Owen MJ. 2002. Early postnatal death and motor disorders in mice congenitally deficient in calnexin expression. Mol Cell Biol 22:7398–7404.

Guo L, Nakamura K, Lynch J, Opas M, Olson EN, Agellon LB, Michalak M. 2002. Cardiac-specific expression of calcineurin reverses embryonic lethality in calreticulin-deficient mouse. J Biol Chem 277:50776–50779.

Hawes C, Osterrieder A, Hummel E, Sparkes I. 2008. The plant ER-Golgi interface. Traffic 9:1571–1580.

Honnappa S, Gouveia SM, Weisbrich A, Damberger FF, Bhavesh NS, Jawhari H, Grigoriev I, van Rijssel FJ, Buey RM, Lawera A, Jelesarov I, Winkler FK, Wüthrich K, Akhmanova A, Steinmetz MO. 2009. An EB1-binding motif acts as a microtubule tip localization signal. Cell 138:366–376.

Hutten S, Kehlenbach RH. 2007. CRM1-mediated nuclear export: To the pore and beyond. Trends Cell Biol 17:193–201.

Jackson MR, Nilsson T, Peterson PA. 1990. Identification of a consensus motif for retention of transmembrane proteins in the endoplasmic reticulum. EMBO J 9:3153–3162.

Leach MR, Williams DB. 2004. Lectin-deficient calnexin is capable of binding class I histocompatibility molecules in vivo and preventing their degradation. J Biol Chem 279:9072–9079.

Li Y, Camacho P. 2004. Ca^{2+}-dependent redox modulation of SERCA 2b by ERp57. J Cell Biol 164:35–46.

Liou J, Kim ML, Heo WD, Jones JT, Myers JW, Ferrell JE, Jr., Meyer T. 2005. STIM is a Ca^{2+} sensor essential for Ca^{2+}-store-depletion-triggered Ca^{2+} influx. Curr Biol 15:1235–1241.

Liou J, Fivaz M, Inoue T, Meyer T. 2007. Live-cell imaging reveals sequential oligomerization and local plasma membrane targeting of stromal interaction molecule 1 after Ca^{2+} store depletion. Proc Natl Acad Sci USA 104:9301–9306.

Luik RM, Wu MM, Buchanan J, Lewis RS. 2006. The elementary unit of store-operated Ca^{2+} entry: Local activation of CRAC channels by STIM1 at ER-plasma membrane junctions. J Cell Biol 174:815–825.

Munro S, Pelham HR. 1987. A C-terminal signal prevents secretion of luminal ER proteins. Cell 48:899–907.

Muromoto R, Ishida M, Sugiyama K, Sekine Y, Oritani K, Shimoda K, Matsuda T. 2006. Sumoylation of Daxx regulates IFN-induced growth suppression of B lymphocytes and the hormone receptor-mediated transactivation. J Immunol 177:1160–1170.

Ni M, Lee AS. 2007. ER chaperones in mammalian development and human diseases. FEBS Lett 581:3641–3651.

Nilsson T, Jackson M, Peterson PA. 1989. Short cytoplasmic sequences serve as retention signals for transmembrane proteins in the endoplasmic reticulum. Cell 58:707–718.

Oda Y, Hosokawa N, Wada I, Nagata K. 2003. EDEM as an acceptor of terminally misfolded glycoproteins released from calnexin. Science 299:1394–1397.

Okada N, Ishigami Y, Suzuki T, Kaneko A, Yasui K, Fukutomi R, Isemura M. 2008. Importins and exportins in cellular differentiation. J Cell Mol Med 12:1863–1871.

Oritani K, Kincade PW. 1996. Identification of stromal cell products that interact with pre-B cells. J Cell Biol 134:771–782.

Park CY, Hoover PJ, Mullins FM, Bachhawat P, Covington ED, Raunser S, Walz T, Garcia KC, Dolmetsch RE, Lewis RS. 2009. STIM1 clusters and activates CRAC channels via direct binding of a cytosolic domain to Orai1. Cell 136:876–890.

Putney JW, Jr. 1986. A model for receptor-regulated calcium entry. Cell Calcium 7:1–12.

Putney JW, Jr. 2007. New molecular players in capacitative Ca^{2+} entry. J Cell Sci 120:1959–1965.

Roos J, DiGregorio PJ, Yeromin AV, Ohlsen K, Lioudyno M, Zhang S, Safrina O, Kozak JA, Wagner SL, Cahalan MD, Veliçelebi G, Stauderman KA. 2005. STIM1, an essential and conserved component of store-operated Ca^{2+} channel function. J Cell Biol 169:435–445.

Sato K, Sato M, Nakano A. 1997. Rer1p as common machinery for the endoplasmic reticulum localization of membrane proteins. Proc Natl Acad Sci USA 94:9693–9698.

Sekine Y, Yamamoto T, Yumioka T, Sugiyama K, Tsuji S, Oritani K, Shimoda K, Minoguchi M, Yoshimura A, Matsuda T. 2005. Physical and fnctional interactions between STAP-2/BKS and STAT5. J Biol Chem 280:8188–8196.

Siomi MC, Eder PS, Kataoka N, Wan L, Liu Q, Dreyfuss G. 1997. Transportin-mediated nuclear import of heterogeneous nuclear RNP proteins. J Cell Biol 138:1181–1192.

Smyth JT, DeHaven WI, Bird GS, Putney JW, Jr. 2007. Role of the microtubule cytoskeleton in the function of the store-operated Ca^{2+} channel activator STIM1. J Cell Sci 120:3762–3771.

Soboloff J, Spassova MA, Hewavitharana T, He LP, Xu W, Johnstone LS, Dziadek MA, Gill DL. 2006a. STIM2 is an inhibitor of STIM1-mediated store-operated Ca^{2+} Entry. Curr Biol 16:1465–1470.

Soboloff J, Spassova MA, Dziadek MA, Gill DL. 2006b. Calcium signals mediated by STIM and Orai proteins—A new paradigm in inter-organelle communication. Biochim Biophys Acta 1763:1161–1168.

Spang A. 2009. On vesicle formation and tethering in the ER-Golgi shuttle. Curr Opin Cell Biol 21:531–536.

Stathopulos PB, Zheng L, Li GY, Plevin MJ, Ikura M. 2008. Structural and mechanistic insights into STIM1-mediated initiation of store-operated calcium entry. Cell 135:110–122.

Vig M, Peinelt C, Beck A, Koomoa DL, Rabah D, Koblan-Huberson M, Kraft S, Turner H, Fleig A, Penner R, Kinet JP. 2006. CRACM1 is a plasma membrane protein essential for store-operated Ca^{2+} entry. Science 312: 1220–1223.

Williams RT, Manji SS, Parker NJ, Hancock MS, Van Stekelenburg L, Eid JP, Senior PV, Kazenwadel JS, Shandala T, Saint R, Smith PJ, Dziadek MA. 2001. Identification and characterization of the STIM (stromal interaction molecule) gene family: Coding for a novel class of transmembrane proteins. Biochem J 357:673–685.

Wu MM, Buchanan J, Luik RM, Lewis RS. 2006. Ca^{2+} store depletion causes STIM1 to accumulate in ER regions closely associated with the plasma membrane. J Cell Biol 174:803–813.

Yuan JP, Zeng W, Dorwart MR, Choi YJ, Worley PF, Muallem S. 2009. SOAR and the polybasic STIM1 domains gate and regulate Orai channels. Nat Cell Biol 11:337–343.

Zhang SL, Yu Y, Roos J, Kozak JA, Deerinck TJ, Ellisman MH, Stauderman KA, Cahalan MD. 2005. STIM1 is a Ca^{2+} sensor that activates CRAC channels and migrates from the Ca^{2+} store to the plasma membrane. Nature 437:902–905.

Zhang SL, Yeromin AV, Zhang XH, Yu Y, Safrina O, Penna A, Roos J, Stauderman KA, Cahalan MD. 2006. Genome-wide RNAi screen of $Ca(2^+)$ influx identifies genes that regulate $Ca(2^+)$ release-activated $Ca(2^+)$ channel activity. Proc Natl Acad Sci USA 103:9357–9362.

blood

2011 117: 250-258
Prepublished online October 12, 2010;
doi:10.1182/blood-2009-10-246751

A potential role for α-actinin in inside-out αIIbβ3 signaling

Seiji Tadokoro, Tsuyoshi Nakazawa, Tsuyoshi Kamae, Kazunobu Kiyomizu, Hirokazu Kashiwagi, Shigenori Honda, Yuzuru Kanakura and Yoshiaki Tomiyama

Blood (print ISSN 0006-4971, online ISSN 1528-0020), is published weekly by the American Society of Hematology, 2021 L St, NW, Suite 900, Washington DC 20036.

A potential role for α-actinin in inside-out αIIbβ3 signaling

Seiji Tadokoro,[1,2] Tsuyoshi Nakazawa,[1] Tsuyoshi Kamae,[1] Kazunobu Kiyomizu,[1] Hirokazu Kashiwagi,[1] Shigenori Honda,[3] Yuzuru Kanakura,[1] and Yoshiaki Tomiyama[1,2]

[1]Department of Hematology and Oncology, Osaka University Graduate School of Medicine C9, Osaka, Japan; [2]Department of Blood Transfusion, Osaka University Hospital, Osaka, Japan; and [3]National Cardiovascular Center Research Institute, Osaka, Japan

Many different biochemical signaling pathways regulate integrin activation through the integrin cytoplasmic tail. Here, we describe a new role for α-actinin in inside-out integrin activation. In resting human platelets, α-actinin was associated with αIIbβ3, whereas inside-out signaling (αIIbβ3 activation signals) from protease-activated receptors (PARs) dephosphorylated and dissociated α-actinin from αIIbβ3. We evaluated the time-dependent changes of the αIIbβ3 activation state by measuring PAC-1 binding velocity. The initial velocity analysis clearly showed that PAR1-activating peptide stimulation induced only transient αIIbβ3 activation, whereas PAR4-activating peptide induced long-lasting αIIbβ3 activation. When αIIbβ3 activation signaling dwindled, α-actinin became rephosphorylated and reassociated with αIIbβ3. Compared with control platelets, the dissociation of α-actinin from αIIbβ3 was only transient in PAR4-stimulated $P2Y_{12}$-deficient platelets in which the sustained αIIbβ3 activation was markedly impaired. Overexpression of wild-type α-actinin, but not the mutant Y12F α-actinin, increased its binding to αIIbβ3 and inhibited PAR1-induced initial αIIbβ3 activation in the human megakaryoblastic cell line, CMK. In contrast, knockdown of α-actinin augmented PAR-induced αIIbβ3 activation in CMK. These observations suggest that α-actinin might play a potential role in setting integrins to a default low-affinity ligand-binding state in resting platelets and regulating αIIbβ3 activation by inside-out signaling. (*Blood.* 2011;117(1):250-258)

Introduction

Integrins and their ligands play key roles in development, immune responses, leukocyte traffic, hemostasis, and cancer and are at the core of numerous human diseases.[1] Many integrins are expressed with their extracellular domains in a default low-affinity ligand-binding state. The main platelet integrin, αIIbβ3, also known as GPIIb/IIIa, is present at a high density on circulating platelets. It is inactive on circulating platelets; if it were not, platelets would bind their main ligand, fibrinogen, from the plasma and aggregate, leading to thrombosis. This inactivation is important for the biologic function of integrins, as is most evident from assessments of their status on circulating blood cells. However, the molecular mechanisms of their being set to an inactive, low-affinity state remain unknown.

High-affinity ligand binding requires activation of integrins through conformational changes regulated by inside-out signaling.[2] Integrin cytoplasmic domains play a pivotal role in integrin signaling because the cytoplasmic tails of the integrin α and β subunits are directly accessible to the intracellular signaling apparatus, namely the integrin activation complex (IAC).[3] Moreover, ligand binding to the integrin induces outside-in signaling that leads to integrin clustering and subsequent recruitment of actin filaments to the integrin cytoplasmic domain. From the perspective that this recruitment occurs by a complex of interacting cytoskeletal proteins, many studies have focused on the components of the IAC, including talin, kindlin, filamin, and α-actinin. The binding of talin to the integrin β subunit cytoplasmic tail is a common final step in the activation process.[4-8] Kindlins bind to the more C-terminal of the NPxY motifs in β-integrin tails and modulate integrin activation.[9-11] Filamin binding to β integrin cytoplasmic tails is competitive with that of talin.[12] Although these studies suggest a model in which multiple proteins jockey for position on the β integrin tail, how cells orchestrate the process remains less well understood.

α-Actinin plays multiple important roles in the cell.[13,14] It links the cytoskeleton to different transmembrane proteins in a variety of junctions, regulates activity of several receptors, and serves as a scaffold connecting the cytoskeleton to diverse signaling pathways. α-Actinin binds to the β integrin cytoplasmic tail,[15,16] and recent studies have shown that the interaction between α-actinin and the integrin β2 tail modulates integrin affinity.[17,18] For regulating α-actinin function, 4 main mechanisms have been identified to date: processing by proteases, binding to phosphatidylinositol intermediaries, phosphorylation by tyrosine kinases, and binding to calcium. For tyrosine phosphorylation regulation, a second wave of protein tyrosine phosphorylation that is strictly dependent on both ligand binding to αIIbβ3 and cytoskeleton organization was observed in platelets stimulated by thrombin, phorbol myristate acetate, or immobilized fibrinogen.[19] Platelet adhesion and spreading on fibrinogen, mediated by the integrin αIIbβ3, trigger a robust and sustained phosphorylation of focal adhesion kinase and α-actinin by outside-in signaling.[20,21] Focal adhesion kinase phosphorylates α-actinin, which lowers its affinity for actin.[22] Dephosphorylation of α-actinin is regulated by the protein tyrosine phosphatase (PTP) SHP-1 (also named PTP1C, SHPTP-1, SHP,

Submitted October 6, 2009; accepted October 1, 2010. Prepublished online as *Blood* First Edition paper, October 12, 2010; DOI 10.1182/blood-2009-10-246751.

The online version of this article contains a data supplement.

The publication costs of this article were defrayed in part by page charge payment. Therefore, and solely to indicate this fact, this article is hereby marked "advertisement" in accordance with 18 USC section 1734.

HCP, and PTPN6),[23] a main PTP expressed in platelets. Although the regulation of α-actinin by outside-in signaling has been well characterized, its role in inside-out signaling remains to be determined.

Here, we show that α-actinin is associated with resting αIIbβ3 in platelets. Inside-out signaling from thrombin receptors, protease-activated receptor 1 (PAR1) and PAR4, dephosphorylated and dissociated α-actinin from αIIbβ3. Protease-activated receptor 1–activating peptide (PAR1-AP) and PAR4-AP induce transient and sustained αIIbβ3 activation, respectively. When the αIIbβ3 activation signaling dwindled, α-actinin reassociated with αIIbβ3 on rephosphorylation. Our observations suggest an emergent picture of α-actinin as having a role in keeping integrins in a default low-affinity ligand-binding state and regulating integrin activation.

Methods

Preparation of human platelets

Platelets were taken from healthy donors as approved by the institutional review board of Osaka University and were prepared as described previously[24] with some modifications. In brief, venous blood was obtained from volunteers with acid citrate dextrose solution (National Institute of Health formula A) as an anticoagulant, used at a 1:6 vol/vol ratio. Platelet-rich plasma was obtained by centrifugation at 250*g* for 10 minutes. After incubation with 0.5μM prostaglandin E_1 for 15 minutes, platelets were isolated by centrifugation of the platelet-rich plasma at 750*g* for 10 minutes. The pellet was washed twice with PIPES (Piperazine-1,4-bis(2-ethanesulfonic acid)) saline buffer (0.15M NaCl, 20mM PIPES, pH 6.5). The washed platelets were resuspended in Walsh buffer (137mM NaCl, 2.7mM KCl, 1mM $MgCl_2$, 3.3mM NaH_2PO4, 3.8mM HEPES [N-2-hydroxyethylpiperazine-N′-2-ethanesulfonic acid], 0.1% glucose, 0.1% bovine serum albumin [BSA], pH 7.4) to a density of 4×10^8 platelets/mL and allowed to sit for 30 minutes before use.

Antibodies

The monoclonal anti–α-actinin antibody (BM-75.2) and anti–talin antibody (8d4) were purchased from Sigma-Aldrich. The monoclonal anti–α-actinin antibody (H-2) and horseradish peroxidase (HRP)–conjugated anti–mouse immunoglobulin M (IgM) were purchased from Santa Cruz Biotechnology. Anti–vasodilator-stimulated phosphoprotein (VASP) monoclonal antibody (IE273) was purchased from ImmunoGlobe. The antiphosphotyrosine (4G10) antibody and anti–phospho-VASP-Ser239 (16C2) were purchased from Upstate Cell Signaling Solutions. PAC-1, the monoclonal, ligand-mimetic, αIIbβ3-specific antibody that binds specifically to activated αIIbβ3, the allophycocyanin-conjugated monoclonal anti-CD25 antibody, allophycocyanin-conjugated anti-CD42b antibody, and phycoerythrin-conjugated anti-CD42b antibody were purchased from BD Biosciences. peridinin chlorophyll protein complex–cyanine 5.5 (PerCP-Cy5.5)–conjugated anti-CD25 antibody was purchased from eBioscience. The polyclonal anti-αIIbβ3 antibody was a gift from Dr Thomas J. Kunicki (The Scripps Research Institute), and the monoclonal anti-αIIbβ3 antibody that activates αIIbβ3, PT25-2,[25] was a gift from Drs. Makoto Handa and Yasuo Ikeda (Keio University). HRP-conjugated secondary antibodies, anti–mouse IgG (H+L), and anti–rabbit IgG (H+L) were purchased from Cell Signaling Technology. Fluorescein isothiocyanate (FITC)– or phycoerythrin-conjugated anti–mouse IgM (μ) was purchased from Caltag Laboratories.

Chemicals

PAR1-AP (SFLLRN), thrombin, and prostaglandin E_1 were purchased from Sigma-Aldrich. PAR4-AP (AYPGKF) was purchased from GenixTalk. AR-C69931MX, a $P2Y_{12}$-specific antagonist, was a gift from Astra-Zeneca. FK633, an αIIbβ3-specific antagonist,[26] was a gift from Astellas Pharma Inc. Protein phosphatase inhibitor-1 (PTPI-1) was purchased from Calbiochem.

Immunoprecipitation

Aliquots of washed platelets (4×10^8/mL) were incubated with PAR1-AP (25μM), PAR4-AP (150μM), or thrombin (0.2 U/mL) at room temperature. Reactions were stopped by lysis of platelets with an equal volume of 2 × neutral detergent lysis buffer (15mM HEPES, 150mM NaCl, 2% [vol/vol] Triton X-100, 10mM EGTA [ethylene glycol tetraacetic acid], and 1mM Na_3VO_4, pH 7.4, plus complete protease inhibitors purchased from Roche Applied Science). Insoluble debris was cleared from the lysate by centrifugation at 13 000*g* for 4 minutes at 4°C. Supernatants were precleared with protein G-sepharose (GE Healthcare) for 1 hour. Precleared lysates were added to the newly prepared protein G with 1 μg of antibody and incubated at 4°C with constant rotation. Immunoprecipitates were washed 3 times, and proteins were eluted from the beads by incubation of the immunoprecipitates with 20 μL of 3 × sodium dodecylsulfate (SDS) sample buffer (62.5mM Tris [tris(hydroxymethyl)aminomethane], pH 6.8, 25% [vol/vol] glycerol, 2% [vol/vol] SDS, 5mM 2-mercaptoethanol, and 0.01% bromophenol blue) at 96°C for 5 minutes.

Electrophoresis of proteins and immunoblotting

Proteins were separated by continuous SDS–polyacrylamide gel electrophoresis on 4%-20% gels and electrophoretically transferred to Immobilon-P phenylmethlsulfonyl fluoride membranes (Millipore). Membranes were blocked by incubation with 2% (wt/vol) BSA in TBST (150mM NaCl, 50mM Tris, and 0.1% [vol/vol] Tween 20, pH 7.4). Primary antibodies were diluted in 2% (wt/vol) BSA in TBST. After incubation with primary antibodies, membranes were washed with TBST and incubated with HRP-conjugated secondary antibodies for 1 hour at room temperature. After further washing of the membrane, signals were detected by enhanced chemiluminescence. When necessary, membranes were immersed in Restore Western blot stripping buffer (Pierce Chemical) and incubated at room temperature for 30 minutes before extensive washing and reprobing with the appropriate antibody.

Cell culture, plasmids, and transfections

Mammalian expression plasmids, including pcDNA/α-actinin, were a gift from Dr Beatrice Haimovich (University of Medicine and Dentistry of New Jersey). The mutant α-actinin carrying a phenylalanine at position 12 (Y12F) was generated as described.[22] CMK cells were maintained in culture as described previously.[27] Ribavirin was not used in this study. The plasmid encoding the extracellular and transmembrane domains of the Tac subunit of the human interleukin-2 receptor was generated as described.[28] Nucleofection was performed with Nucleofector II (Amaxa Biosystems) according to the manufacturer's instructions. CMK cells were nucleofected with 10 μg/cuvette Tac subunit of the human interleukin-2 receptor–encoding plasmid and 20 μg/cuvette α-actinin–encoding plasmid. Cells were analyzed 20 hours after nucleofection. The short hairpin RNAs (shRNAs) lentiviral particules were generated as described.[4] 5′-GGAAGCCAGGCATGTGGTTCTGATCATTGG AAGCTTGCGATGATTAGGACTACATGCCTGTCTTCCTTTTTT-3′ and 5′-GGCCAGCTTCTCGTAGTCTTCCATAAGCTGAAGCTT GAGCTTATGGAGGATTATGAGAAGCTGGCTTTTTTT-3′ oligonucleotide sequences were used to construct control and α-actinin shRNA, respectively. The α-actinin shRNA sequence chosen is specific for human α-actinin-1 and is 82% conserved in the human α-actinin-4 nucleotide sequence. shRNA viral vectors were produced by cloning the siRNA cassette into the FG12 lentiviral transgene vector in which DsRed2 was substituted for enhanced green fluorescent protein. In plasmids encoding wild-type or mutant α-actinin, 3 silence mutations were generated to prevent annealing with the α-actinin shRNA.

Flow cytometry and platelet aggregometry

Aliquots of washed platelets and FITC–PAC-1 were incubated with PAR1-AP (25μM), PAR4-AP (150μM), or thrombin (0.2 U/mL) at room temperature for various times. Binding of PAC-1 to platelets or CMK cells was assessed by flow cytometry with the use of FACSCalibur (Becton Dickinson).[29] The initial velocity of bound PAC-1 was analyzed as

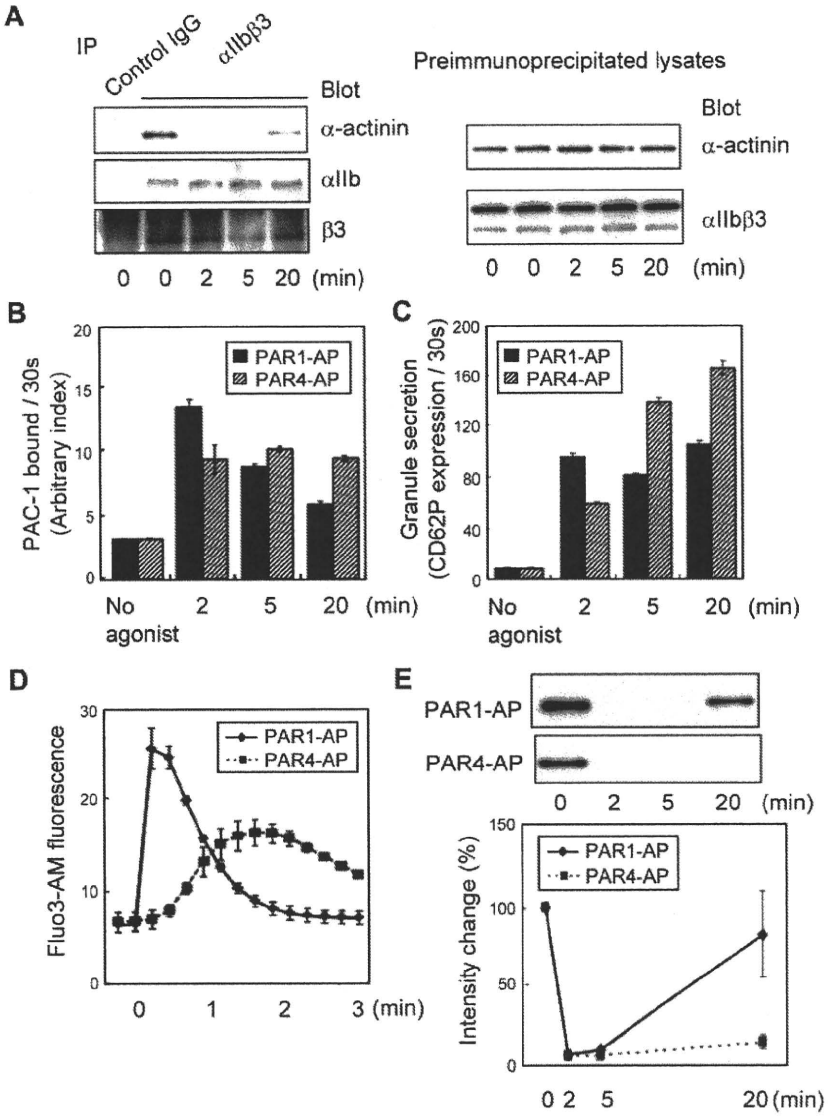

Figure 1. Dynamic changes in the interaction between αIIbβ3 and α-actinin in platelets. Washed human platelets were stimulated with PAR1-AP (25μM) or PAR4-AP (150μM) under nonstirring conditions for the time indicated. (A) αIIbβ3 was immunoprecipitated from lysates prepared from human platelets stimulated with PAR1-AP. Immunoprecipitates were then subjected to SDS–polyacrylamide gel electrophoresis (PAGE) and immunoblotted with anti–α-actinin antibody. Immunoblots were stripped and reprobed with anti-αIIbβ3 antibody. Preimmunoprecipitated lysates were also subjected to SDS-PAGE and immunoblotted with the same series of antibodies. (B) FITC–PAC-1 was added to the activated platelets after stimulation and incubated for 30 seconds to obtain the PAC-1 binding velocity at the time indicated. PAC-1 binding/30 seconds was normalized for integrin expression levels. (C) Phycoerythrin-conjugated anti-CD62P was added to the activated platelets and incubated for only 30 seconds to evaluate granule secretion. (D) Intracellular calcium mobilization was assessed by monitoring Fluo3-AM fluorescence by flow cytometry. (E) αIIbβ3 was immunoprecipitated then immunoblotted with anti–α-actinin antibody. Immunoblots shown are representative of 3 different experiments and analyzed by scanning densitometry and quantified with ImageJ (National Institutes of Health).

described.[30] In brief, washed platelets were mixed with PAR-AP at time "zero." At different time points from 2 minutes to 20 minutes, 20 μL of FITC–PAC-1 was added, and 30 seconds after the addition of PAC-1, 50 μL of platelet suspension was diluted into Walsh buffer, and bound PAC-1 was measured by flow cytometry. PAR1-AP–induced PAC-1 binding to CMK cells was analyzed on a gated subset of live (propidium iodide negative) differentiated (strongly $CD42b^+$) transfected (strongly $CD25^+$ or $DsRed2^+$) cells. Specific binding was assessed as total binding minus binding in the presence of 10μM FK633. Intracellular α-actinin expression was assessed by flow cytometry as previously described.[4] In brief, CMK cells were fixed with 0.5% paraformaldehyde, permeabilized with 0.05% saponin, and incubated for 30 minutes at room temperature with anti–α-actinin monoclonal antibody. After washing, the cells were incubated another 30 minutes with FITC-conjugated goat anti–mouse IgM. Cells were washed and resuspended in 500 μL of phosphate-buffered saline then analyzed by flow cytometry.

Presentation of data

Data are presented as mean ± SEM of ≥ 3 individual experiments from different blood donors. Analysis of statistical significance was performed with Student paired *t* tests, and differences were considered significant when $P < .05$. Immunoblots shown are representatives of 3 different experiments and were analyzed by scanning densitometry and quantified with ImageJ Version 1.40g (National Institutes of Health).

Results

Dynamic changes in the interaction between αIIbβ3 and α-actinin in platelets

Human washed platelets were stimulated with 25μM PAR1-AP under nonstirring conditions for ≤ 20 minutes to explore the role of α-actinin in inside-out signaling. Immunoprecipitation with polyclonal anti-αIIbβ3 followed by immunoblotting with anti–α-actinin showed that, in resting platelets, α-actinin was already associated with resting αIIbβ3 (Figure 1A). When platelets were stimulated with PAR1-AP, α-actinin was dissociated from αIIbβ3. Some actin-binding proteins moved to the Triton X-100–insoluble

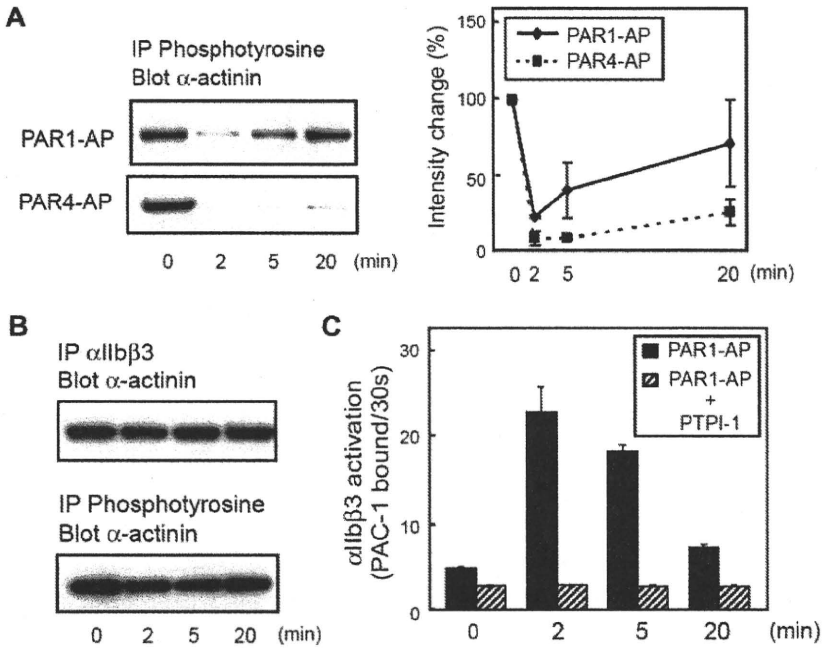

Figure 2. Kinetics of tyrosine phosphorylation of α-actinin during platelet activation and inhibition of SHP-1 by PTPI-1. Washed human platelets were stimulated with PAR1-AP (25μM) or PAR4-AP (150μM) for the time indicated. (A) Tyrosine-phosphorylated proteins were immunoprecipitated then immunoblotted with anti–α-actinin antibody. Immunoblots were analyzed by scanning densitometry and were quantified with ImageJ. (B) Washed human platelets were incubated at room temperature for 2 minutes in the presence of PTPI-1 (50μM). The platelets were then stimulated with PAR1-AP (25μM) for the time indicated. αIIbβ3 or tyrosine-phosphorylated proteins were immunoprecipitated then immunoblotted with anti–α-actinin antibody. (C) FITC–PAC-1 was added to the activated platelets after stimulation and incubated for 30 seconds to obtain the PAC-1 binding velocity at the time indicated. Error bars represent SEMs of 3 experiments.

fraction from the Triton X-100–soluble fraction in response to platelet activation; however, the amounts of α-actinin, talin, and αIIbβ3 in the Triton X-100–soluble fraction of PAR1-AP–activated platelets were similar to those of resting platelets under our experimental conditions. This finding suggests that the dissociation was not the result of the translocation of α-actinin into the Triton X-100–insoluble fraction. This dissociation remained unaffected even in the presence of 10μM of the αIIbβ3-specific peptidomimetic antagonist FK633, suggesting that the dissociation is independent of αIIbβ3-mediated outside-in signaling (data not shown). Interestingly, α-actinin rebound to αIIbβ3 at 20 minutes after PAR1-AP stimulation.

To clarify the physiologic relevance of the α-actinin dissociation to αIIbβ3 activation, we measured the amounts of PAC-1 binding after PAR1-AP or PAR4-AP stimulation. FITC–PAC-1 was incubated with activated platelets for 2 minutes, 5 minutes, and 20 minutes. Under PAR4-AP stimulation, the levels of PAC-1 binding increased as the incubation time extended. However, with PAR1-AP stimulation, the level of PAC-1 binding for a 20-minute incubation was similar to (or even lower than) that for a 5-minute incubation, suggesting that the number of activated αIIbβ3 molecules decreased at 20 minutes after PAR1-AP stimulation (supplemental Figure 1A, available on the *Blood* Web site; see the Supplemental Materials link at the top of the online article).

To evaluate more precisely the dynamic changes in the αIIbβ3 activation state, we performed initial velocity analysis for PAC-1 binding that has recently been developed.[30] In brief, FITC–PAC-1 was added to the activated platelets at the indicated time points after stimulation and incubated for only 30 seconds to obtain the PAC-1 binding velocity at the time points in question. The velocity of PAC-1 binding reflects the relative numbers of activated αIIbβ3 at those time points. PAC-1 binding was normalized for integrin expression levels. This initial velocity analysis clearly showed that PAR1 stimulation induced only transient αIIbβ3 activation, whereas PAR4 induced long-lasting αIIbβ3 activation (Figure 1B). Moreover, we assessed granule secretion and calcium mobilization under these conditions. These agonists induced different kinetics in CD62P expression and intracellular calcium mobilization, as detected by Fluo3-AM fluorescence (Figure 1C-D). These characteristics are consistent with the observed transient and sustained αIIbβ3 activation induced by PAR1-AP and PAR4-AP, respectively (Figure 1E). These data suggest that the dissociation of α-actinin may be related to αIIbβ3 activation.

Tyrosine phosphorylation of α-actinin regulates the interaction between α-actinin and αIIbβ3 in platelets

Because the α-actinin function appears to be regulated, in part, by tyrosine phosphorylation, we then examined the tyrosine phosphorylation state of α-actinin. The tyrosine-phosphorylated α-actinin was detectable as a faint band by immunoprecipitation with α-actinin antibody (BM-75.2 or H-2) followed by immunoblotting with 4G10 (supplemental Figure 1B). Accordingly, we modified our methods, and the platelet lysate was first subjected to immunoprecipitation with monoclonal antibody 4G10, followed by immunoblotting with anti–α-actinin antibody. In resting platelets, the anti–α-actinin antibody recognized the single 105-kDa protein (Figure 2A; supplemental Figure 1C). When stimulated with PAR1-AP, α-actinin was rapidly dephosphorylated. Although we have not excluded that this band was coprecipitated α-actinin with phosphoproteins, the phosphorylation profiles of immunoprecipitated α-actinin were almost the same as the faint band at 105 kDa in supplemental Figure 1B, suggesting that α-actinin itself was phosphorylated. α-Actinin was rephosphorylated at 20 minutes after PAR1-AP stimulation, whereas PAR4-AP induced sustained dephosphorylation of α-actinin. In addition to these agonists, we also examined adenosine diphosphate (ADP) and U46619-induced αIIbβ3 activation (supplemental Figure 2). ADP and U46619 induced transient and sustained αIIbβ3 activation, respectively. Again, α-actinin dissociation and de-phosphorylation induced by ADP and U46619 were transient and sustained, respectively. Thus, the kinetics of α-actinin phosphorylation seemed to synchronize with its interaction with αIIbβ3 (Figures 1E,2A).

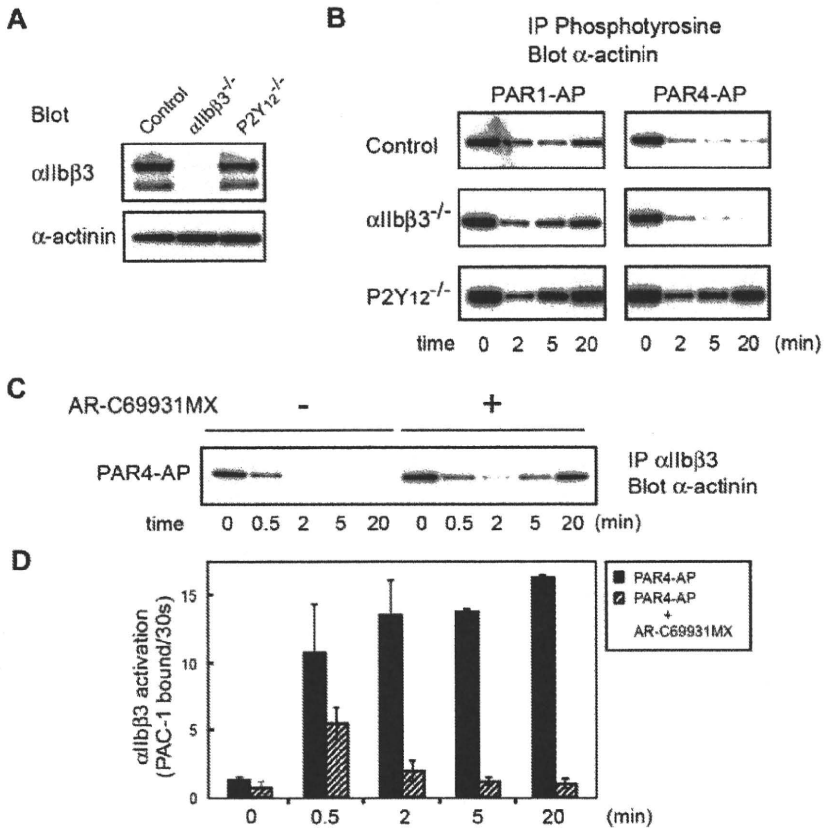

Figure 3. Changes in α-actinin phosphorylation and its interaction with αIIbβ3 in platelets from patients with Glanzmann thrombasthenia or $P2Y_{12}$ deficiency. (A) Platelet lysates from patients with Glanzmann thrombasthenia or patients with $P2Y_{12}$ deficiency were subjected to SDS–polyacrylamide gel electrophoresis and immunoblotted with anti-αIIbβ3 antibody or anti–α-actinin antibody. (B) Washed platelets were stimulated with PAR1-AP (25μM) or PAR4-AP (150μM) for the time indicated. Tyrosine-phosphorylated proteins were immunoprecipitated then immunoblotted with anti–α-actinin antibody. (C) Washed normal platelets were stimulated with PAR4-AP (150μM) for the time indicated after incubation with AR-C69931MX (1μM) for 2 minutes. αIIbβ3 was immunoprecipitated then immunoblotted with anti–α-actinin antibody. (D) Washed normal platelets were stimulated with PAR4-AP (150μM) for the time indicated after incubation with AR-C69931MX (1μM) for 2 minutes. FITC–PAC-1 was added to the activated platelets after stimulation and incubated for 30 seconds to obtain the PAC-1 binding velocity at the time indicated. Error bars represent SEMs of 3 experiments.

It has been shown that the PTP SHP-1 regulates the dephosphorylation of α-actinin.[23] To examine whether dephosphorylation of α-actinin regulates the dissociation of α-actinin from αIIbβ3 and integrin activation, we examined the effects of PTPI-1, a specific inhibitor of SHP-1[31] and PTP1B. Figure 2B shows that PTPI-1 inhibited the dephosphorylation of α-actinin. In addition, PTPI-1 markedly inhibited the activation of αIIbβ3 as well as the dissociation of α-actinin (Figure 2C). These results suggest that tyrosine phosphorylation of α-actinin regulates the interaction between α-actinin and αIIbβ3.

Interaction between α-actinin and integrin in platelets from a patient with Glanzmann thrombasthenia or $P2Y_{12}$ deficiency

To examine further the role of α-actinin in inside-out signaling, we analyzed platelets from a patient with Glanzmann thrombasthenia or $P2Y_{12}$-ADP receptor deficiency.[24] Figure 3A shows the expression profiles of αIIbβ3 and α-actinin in both patients. In Glanzmann thrombasthenia platelets, the phosphotyrosine profile of α-actinin was almost the same as that of control platelets under both PAR1-AP and PAR4-AP stimulation, confirming that αIIbβ3 outside-in signaling does not mediate these changes. In sharp contrast, PAR4-AP stimulation failed to induce the sustained dephosphorylation of α-actinin in $P2Y_{12}$-deficient platelets. Similarly, compared with control platelets, dephosphorylation of α-actinin induced by PAR1-AP was also disrupted at earlier time points in $P2Y_{12}$-deficient platelets (Figure 3B). This early disruption of the dephosphorylation of α-actinin is consistent with our previous finding that $P2Y_{12}$-mediated signaling is essential for sustained αIIbβ3 activation.[29] Indeed, the blockade of $P2Y_{12}$ with AR-C69931MX impaired the PAR4-AP–induced sustained αIIbβ3 activation, leading to the reassociation of α-actinin with αIIbβ3 (Figure 3C-D).

We have previously reported that the sustained αIIbβ3 activation induced by thrombin could be disrupted by inhibiting $P2Y_{12}$-mediated signaling even after thrombin stimulation.[29] Washed platelets were stimulated with thrombin at 0.2 U/mL. Two minutes later, we added AR-C69931MX (1μM) to the thrombin-stimulated platelets. We confirmed that AR-C69931MX still disrupted the sustained αIIbβ3 activation even under these conditions (Figure 4A). Interestingly, the sustained dephosphorylation and the dissociation of α-actinin from αIIbβ3 were disrupted by adding AR-C69931MX (Figure 4B-C). The blockade of $P2Y_{12}$ was confirmed by the VASP phosphorylation state.[32] These results suggest that the interaction between α-actinin and αIIbβ3 is, at least in part, regulated by $P2Y_{12}$-mediated signaling but not by αIIbβ3 outside-in signaling.

α-Actinin modulates agonist-induced αIIbβ3 activation in CMK cells

Finally, we used direct genetic manipulation to examine the effect of α-actinin on αIIbβ3 activation in human megakaryoblastic cell line CMK cells. Because the tyrosine residue at position 12 was reported as the main site of tyrosine phosphorylation in α-actinin,[23] we overexpressed wild-type α-actinin and Y12F α-actinin in CMK cells. As shown in Figure 5A, the expression of α-actinin was increased to 130%-170% of endogenous levels without affecting αIIbβ3 expression. Next, we examined the interaction between α-actinin and αIIbβ3 in CMK cells. Like platelets and primary megakaryocytes,[4] CMK cells can activate αIIbβ3 by the stimulation of physiologic agonists such as PAR1-AP.[27,30] Similar to platelets, α-actinin was associated with αIIbβ3 in unstimulated CMK cells. When stimulated with PAR1-AP, α-actinin dissociated from αIIbβ3. Overexpression of wild-type α-actinin, but not the

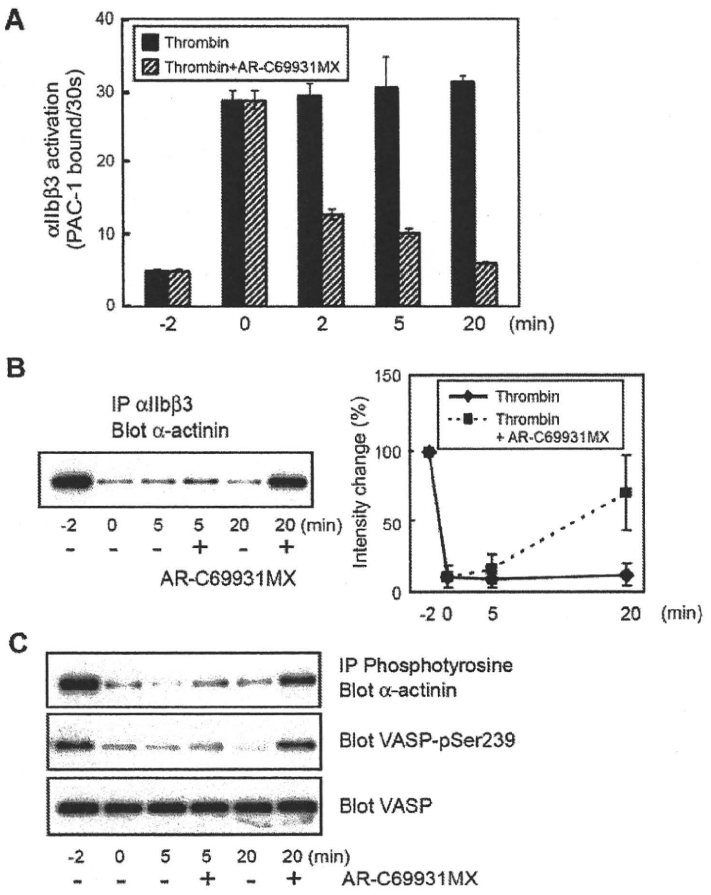

Figure 4. Effects of the blockade of $P2Y_{12}$ on α-actinin and αIIbβ3. Washed human platelets were incubated with thrombin (0.2 U/mL). The $P2Y_{12}$ antagonist, AR-C69931MX (1μM), was added after 2 minutes of thrombin stimulation. (A) FITC–PAC-1 was added to the activated platelets after stimulation and incubated for 30 seconds to obtain the PAC-1 binding velocity at the time indicated. (B) αIIbβ3 was immunoprecipitated then immunoblotted with anti–α-actinin antibody. (C) Tyrosine-phosphorylated proteins were immunoprecipitated then immunoblotted with anti–α-actinin antibody. Preimmunoprecipitated lysates were also subjected to SDS–polyacrylamide gel electrophoresis and immunoblotted with anti–phospho-VASP (Ser239) antibody or anti-VASP antibody. Error bars represent SEMs of 3 experiments.

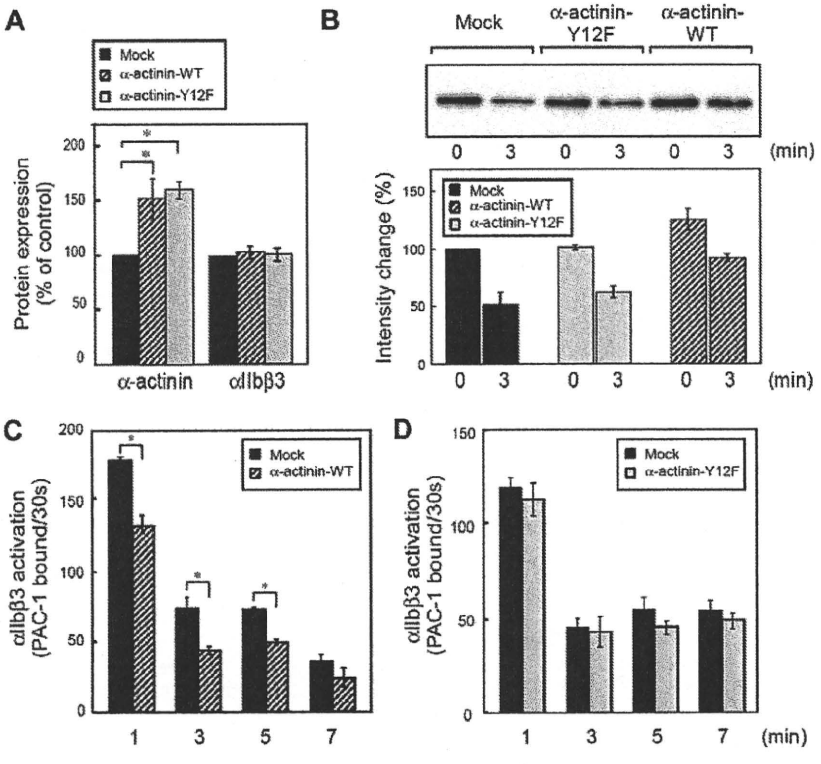

Figure 5. Effects of α-actinin on αIIbβ3 inside-out signaling in CMK cells. Human megakaryoblastic CMK cells were transiently transfected with plasmids encoding for α-actinin and Tac subunit of the human interleukin-2 receptor. Protein expression and integrin activation were assessed 20 hours after transfection. (A) Intracellular α-actinin and surface αIIbβ3 were determined by flow cytometry. Bar charts represent specific antibody binding to highly transfected cells (CD25-allophycocyanin fluorescence > 50) normalized to mock plasmid (pcDNA3.1)–transfected cells. Transfected CMK cells were incubated with PAR1-AP (50μM) for the time indicated. αIIbβ3 was immunoprecipitated then immunoblotted with anti–α-actinin antibody(B). Bar charts represent PAC-1 binding to wild-type α-actinin (C) or mutant α-actinin (D) transfected cells. Error bars represent SEMs of 3 experiments. *$P < .05$.

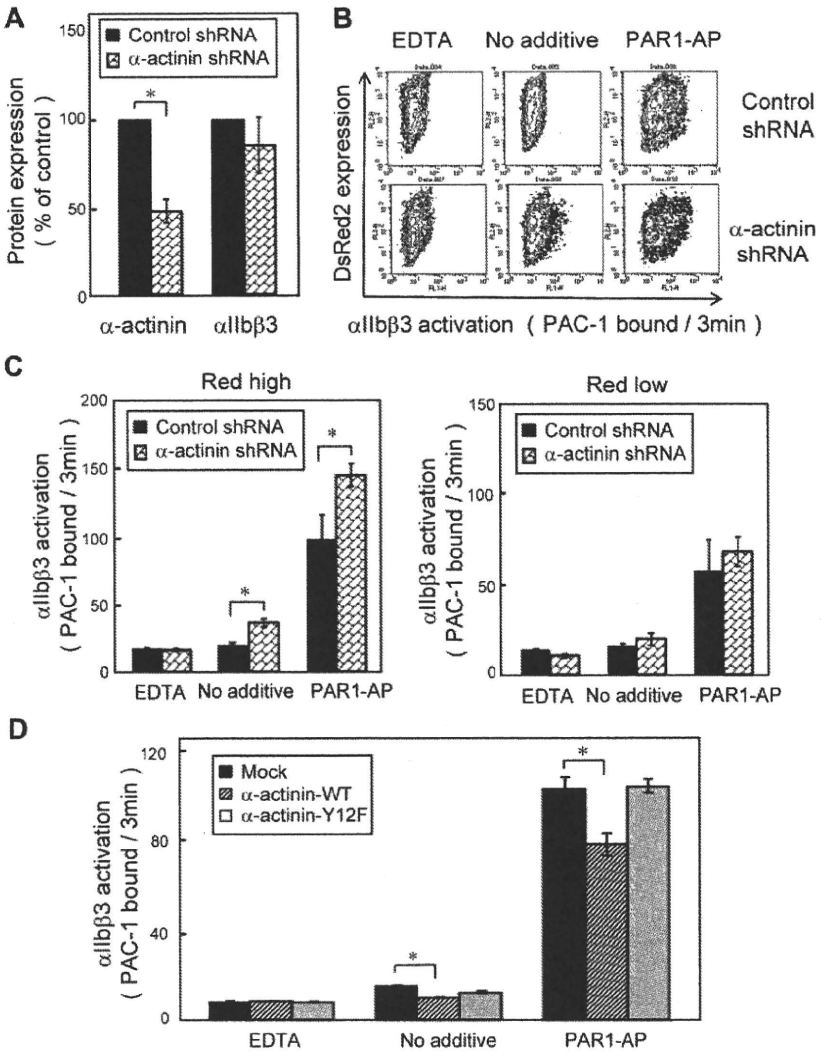

Figure 6. Knockdown of α-actinin augmented PAR1-AP–induced PAC-1 binding in CMK. Lentiviral particles encoding a shRNA for α-actinin or a control shRNA were transduced to CMK cells. (A) Intracellular α-actinin and surface αIIbβ3 were determined by flow cytometry. (B) CMK cells were stimulated with PAR1-AP (50μM) under nonstirring conditions with FITC–PAC-1 for 3 minutes. In contour plots, PAC-1 binding is shown on the x-axis, and transduction of the lentiviral particles is estimated by DsRed2 expression on the y-axis. (C) Bar charts represent PAC-1 binding to highly transduced cells (DsRed2 fluorescence > 250) and to less transduced cells (DsRed2 fluorescence < 50). (D) α-Actinin shRNA–transduced CMK cells were transiently transfected with plasmid encoding for wild-type or mutant α-actinin. Cells were stimulated with PAR1-AP (50μM) under nonstirring conditions with FITC–PAC-1 for 3 minutes. Error bars represent SEMs of 3 experiments in PAR1-AP and EDTA and of 8 experiments in no additive condition. $^*P < .05$.

mutant Y12F α-actinin, increased the basal association between α-actinin and αIIbβ3 (Figure 5B).

We then performed PAC-1 binding velocity analysis on the gated subset of live, transfected, and CD42b$^+$ CMK cells stimulated with PAR1-AP, as described in the experimental procedures. CMK cells bound little PAC-1 in the absence of agonists. When stimulated with PAR1-AP, most mock-transfected cells bound PAC-1 (supplemental Figure 3A). Overexpression of wild-type α-actinin decreased PAC-1 binding velocity (Figure 5C) as well as the amounts of PAC-1 binding in the conventional PAC-1 binding assay (supplemental Figure 3C). The α-actinin expression has a concentration-dependent effect. High expression of α-actinin suppressed PAC-1 binding induced by PAR1-AP, but low expression of α-actinin did not (supplemental Figure 3B). In contrast, overexpression of the mutant Y12F α-actinin did not decrease PAC-1 binding velocity (Figure 5D). To examine further the effects of α-actinin, α-actinin expression was knocked down by shRNA in CMK cells. Knockdown was maximal at 10 days after infection, and shRNA induced 40%-60% reduction in the α-actinin expression (Figure 6A). Although adequate α-actinin reduction may not be obtained in CMK cells, decreased level of α-actinin augmented αIIbβ3 activation induced by PAR1-AP. Again, transduction levels (DsRed2 expression) have a concentration-dependent effect. High expression of DsRed2 augmented PAC-1 binding induced by PAR1-AP, but low expression of DsRed2 did not (Figure 6B-C). In contrast to PAR1-AP, PAR4-AP induced little PAC-1 binding velocity in CMK cells when stimulated with such high concentration as 1mM (supplemental Figure 4A). We assessed whether knockdown of α-actinin affects this PAR4-AP condition in CMK. PAC-1 binding induced by PAR4-AP was significantly augmented in the knockdown cells as well as PAR1-AP (supplemental Figure 4B). Finally wild-type α-actinin and Y12F α-actinin were overexpressed in α-actinin shRNA-transduced CMK cells. Wild-type α-actinin, but not the mutant Y12F α-actinin, normalized the augmented αIIbβ3 activation induced by PAR1-AP in CMK cells (Figure 6D). These results suggest that the binding of α-actinin might be involved in αIIbβ3 activation.

Discussion

Here, we focused on α-actinin as a member of the IAC and assessed its potential role in integrin-reversible activation. Resting αIIbβ3 was already associated with α-actinin, and inside-out

signaling by PARs induced a dissociation of α-actinin from αIIbβ3. This dissociation was regulated by dephosphorylation of α-actinin and associated with reversible αIIbβ3 activation, as evidenced by the stimulation of PAR1-AP and PAR4-AP. Overexpression of wild-type α-actinin, but not a mutant with a tyrosine-phosphorylation defect (Y12F), inhibited αIIbβ3 activation in a megakaryocytic cell line, CMK, in which αIIbβ3 is activated by PAR1-AP. Knockdown of α-actinin augmented PAR-AP–induced PAC-1 binding in CMK. Thus, our observations suggest that α-actinin may play a role in keeping αIIbβ3 in a low-affinity state.

Thrombin activates human platelets through proteolytic activation of 2 protease-activated receptors, PAR1 and PAR4.[33] PAR1 is a high-affinity receptor for platelet activation at low concentrations of thrombin, whereas PAR4 is a low-affinity receptor that mediates thrombin signaling at high concentrations. Consistent with previous reports,[34,35] we showed distinct kinetics of signaling from these PARs by evaluation of intracellular calcium mobilization and P-selectin translocation. PAR1 triggered a rapid and transient increase in intracellular calcium, whereas PAR4 triggered a slower but more prolonged response. Accordingly, we used PAR1-AP and PAR4-AP to examine the role of α-actinin in integrin activation. To assess the activation state of αIIbβ3 more precisely, we performed initial velocity analysis at a specific time point. The kinetic approach with the use of flow cytometry has been proposed for assessing the dynamics of αIIbβ3 activation,[36] and we have modified it as the initial velocity analysis for assessing reversible αIIbβ3 activation. On-rate of PAC-1 binding reflects the number of activated receptors, and the initial velocity analysis showed that PAR1 stimulation induced only transient activation. In addition, only 25% of αIIbβ3 was kept activated at 20 minutes after stimulation compared with the amount of activated αIIbβ3 at 2 minutes after stimulation.

In contrast, PAR4 induced long-lasting αIIbβ3 activation, and the amount of activated αIIbβ3 was almost the same at 2 minutes and 20 minutes after stimulation. The association/dissociation behavior of α-actinin with αIIbβ3 is apparently related to the distinct αIIbβ3 activation kinetics induced by PAR1-AP, PAR4-AP, ADP, and U46619.

We have shown that continuous interaction between released endogenous ADP and $P2Y_{12}$ is critical for sustained αIIbβ3 activation induced by thrombin.[29] In this context, the sustained αIIbβ3 activation induced by PAR4-AP was markedly impaired in $P2Y_{12}$-deficient platelets. In addition, the dissociation and dephosphorylation of α-actinin induced by PAR4-AP as well as by PAR1-AP was markedly impaired. Moreover, after αIIbβ3 activation was completed by thrombin stimulation, the addition of AR-C69931MX disrupted the dissociation and dephosphorylation of α-actinin as well as the sustained αIIbβ3 activation. PTPI-1, an inhibitor of SHP-1, inhibited the dissociation as well as the dephosphorylation of α-actinin induced by PAR1-AP. These data suggest a close association between the dissociation and dephosphorylation of α-actinin and regulation of these changes, at least in part, by $P2Y_{12}$-mediated signaling.

Cellular control of integrin activation requires transmission of a signal from the cytoplasmic tails to the extracellular domains. One may argue that the activation state of αIIbβ3 is an intrinsic state of the integrin itself and not a property of platelets per se.[37] However, this concept is based on the property of exogenous αIIbβ3 expressed on Chinese hamster ovary cells which is not activated by several platelet agonists. In this study, we have demonstrated that endogenous αIIbβ3 expressed on CMK cells can be activated by PAR-APs. Recent studies have identified some intracellular adapters, enzymes, and substrates necessary for αIIbβ3 activation and the tails function as regulatory scaffolds.[38] Among cytoplasmic proteins associated with β3 tail, talin[4,8] and kindlins[9] are now well established as being essential for integrin activation. Recently, it has been shown that talin binding is sufficient to activate integrin αIIbβ3[39] and that a talin membrane contact would be required for integrin activation.[39,40] In this context, α-actinin may modulate the accessibility of talin to the β3 tail or to plasma membrane because putative α-actinin binding sites have been reported within the membrane proximal region of the β3 cytoplasmic tail.[15,41] In platelets α-actinin was no longer associated with αIIbβ3 after PAR-AP stimulation. This may imply that α-actinin knockdown would not further enhance the extent of integrin activation. However, α-actinin knockdown significantly augmented PAC-1 binding induced by 1mM PAR4-AP as well as 50μM PAR1-AP in CMK. Unlike platelets, CMK needed a higher concentration of agonists to get enough levels of activated αIIbβ3. Even under those conditions, the levels of activated αIIbβ3 were less, and the sustained time of activation was shorter than platelets. From these observations, we assume that αIIbβ3 in CMK cells under our experimental conditions may not be fully activated. It is possible that this is the reason why α-actinin knockdown further enhances integrin activation in CMK cells. Thus, the α-actinin binding to the β3 tail may keep αIIbβ3 in a low-affinity state, and it is possible that the dissociation of α-actinin from the β3 tail may lead to the easy accessibility of talin to the β3 tail by inside-out signaling. Like β3 integrin, β2 integrins can change affinity on a subsecond time scale.[1] Recent studies have shown that intermediate-affinity lymphocyte function-associated antigen-1 bound to α-actinin, whereas high-affinity lymphocyte function antigen-1 bound to talin.[17,18] These data show that α-actinin and talin regulate integrin activation differently.

α-Actinin colocalizes with actin and stabilizes the actin filament web in nonmuscle cells.[13] It has been suggested that most α-actinin forms a bridge between the actin filaments and that there is some α-actinin associated with integrin at the end of actin filaments.[14] Indeed, we have confirmed that most α-actinin was not associated with αIIbβ3, as evidenced by the presence of large amounts of α-actinin in the supernatant even in immunoprecipitates of αIIbβ3 from resting platelets (data not shown). In the fibroblast, the phosphorylation of α-actinin reduces its affinity for actin and prevents its localization to focal adhesion plaques.[42] Another report showed that the phosphorylation of α-actinin might serve to modulate the coupling/uncoupling of integrins to the cytoskeleton in platelets.[23] Outside-in signaling involving interaction of αIIbβ3 with its immobilized ligand fibrinogen triggers tyrosine phosphorylation and cytoskeletal reorganization in platelets.[20] Pathologic shear forces, such as those encountered in stenotic midsized coronary and cerebral arteries, directly affect ligand-dependent αIIbβ3 outside-in signaling, and a recent study showed that pathologic shear stress induced dissociation of α-actinin from the β3 tail, which is αIIbβ3 dependent.[43] Our observations described here are clearly different phenomena from those induced by outside-in signaling; an αIIbβ3-specific antagonist, FK633, did not inhibit the dissociation, and dephosphorylation was induced even in thrombasthenic platelets. Thus, both inside-out signaling and outside-in signaling regulate the dissociation of α-actinin from αIIbβ3.

Integrin function is a complex process regulated by the balance of positive and negative regulatory proteins. Several factors have been identified as positive and negative regulators of αIIbβ3.[44,45] Platelet agonists, such as thrombin and ADP, induce αIIbβ3 activation, whereas various vasodilators released from the endothelial cells keep αIIbβ3 inactive in circulating blood. In addition to platelet agonists and vasodilators, the balance of positive and negative

regulatory proteins in IAC may regulate αIIbβ3 activation. Our observations described here suggest that α-actinin may act as a negative regulator in resting platelets. Although further work is needed to determine each specific role of α-actinin in platelets, the α-actinin–integrin interaction might be added to the discussion of new potential targets for atherothrombotic disease therapies.

Acknowledgments

This work was supported by Grant-in Aid for Scientific Research from the Ministry of Education, Culture, Sports, Science and Technology in Japan, from the Ministry of Health, Labor and Welfare in Japan; and "Academic Frontier" Project in Japan.

Authorship

Contribution: S.T. designed and performed experiments, analyzed data, and wrote the paper; T.N., T.K., and K.K. helped perform parts of the experiments; H.K. and S.H. provided feedback and experimental advice; and Y.K. and Y.T. supervised the project and reviewed the paper.

Conflict-of-interest disclosure: The authors declare no competing financial interests.

Correspondence: Seiji Tadokoro, Department of Hematology and Oncology, Osaka University Graduate School of Medicine C9, 2-2 Yamada-oka, Suita Osaka 565-0871, Japan; e-mail: tadokoro@hp-blood.med.osaka-u.ac.jp.

References

1. Hynes RO. Integrins: bidirectional, allosteric signaling machines. *Cell.* 2002;110(6):673-687.
2. Shattil SJ, Newman PJ. Integrins: dynamic scaffolds for adhesion and signaling in platelets. *Blood.* 2004;104(6):1606-1615.
3. O'Toole TE, Katagiri Y, Faull RJ, et al. Integrin cytoplasmic domains mediate inside-out signal transduction. *J Cell Biol.* 1994;124(6):1047-1059.
4. Tadokoro S, Shattil SJ, Eto K, et al. Talin binding to integrin beta tails: a final common step in integrin activation. *Science.* 2003;302(5642):103-106.
5. Moser M, Legate KR, Zent R, Fässler R. The tail of integrins, talin, and kindlins. *Science.* 2009; 324(5929):895-899.
6. Wegener KL, Partridge AW, Han J, et al. Structural basis of integrin activation by talin. *Cell.* 2007;128(1):171-182.
7. Petrich BG, Marchese P, Ruggeri ZM, et al. Talin is required for integrin-mediated platelet function in hemostasis and thrombosis. *J Exp Med.* 2007; 204(13):3103-3111.
8. Nieswandt B, Moser M, Pleines I, et al. Loss of talin1 in platelets abrogates integrin activation, platelet aggregation, and thrombus formation in vitro and in vivo. *J Exp Med.* 2007;204(13):3113-3118.
9. Moser M, Nieswandt B, Ussar S, Pozgajova M, Fässler R. Kindlin-3 is essential for integrin activation and platelet aggregation. *Nat Med.* 2008; 14(3):325-330.
10. Ma YQ, Qin J, Wu C, Plow EF. Kindlin-2 (Mig-2): a co-activator of beta3 integrins. *J Cell Biol.* 2008; 181(3):439-446.
11. Harburger DS, Bouaouina M, Calderwood DA. Kindlin-1 and -2 directly bind the C-terminal region of beta integrin cytoplasmic tails and exert integrin-specific activation effects. *J Biol Chem.* 2009;284(17):11485-11497.
12. Kiema T, Lad Y, Jiang P, et al. The molecular basis of filamin binding to integrins and competition with talin. *Mol Cell.* 2006;21(3):337-347.
13. Otey CA, Carpen O. alpha-Actinin revisited: a fresh look at an old player. *Cell Motil Cytoskeleton.* 2004;58(2):104-111.
14. Sjöblom B, Salmazo A, Djinović-Carugo K. alpha-Actinin structure and regulation. *Cell Mol Life Sci.* 2008;65(17):2688-2701.
15. Otey CA, Pavalko FM, Burridge K. An interaction between alpha-actinin and the beta1 integrin subunit in vitro. *J Cell Biol.* 1990;111(2):721-729.
16. Pavalko FM, LaRoche SM. Activation of human neutrophils induces an interaction between the integrin beta2-subunit (CD18) and the actin binding protein alpha-actinin. *J Immunol.* 1993;151(7):3795-3807.
17. Smith A, Carrasco YR, Stanley P, Kieffer N, Batista FD, Hogg N. A talin-dependent LFA-1 focal zone is formed by rapidly migrating T lymphocytes. *J Cell Biol.* 2005;170(1):141-151.
18. Stanley P, Smith A, McDowall A, Nicol A, Zicha D, Hogg N. Intermediate-affinity LFA-1 binds alpha-actinin-1 to control migration at the leading edge of the T cell. *EMBO J.* 2008;27(1):62-75.
19. Shattil SJ, Ginsberg MH, Brugge JS. Adhesive signaling in platelets. *Curr Opin Cell Biol.* 1994; 6(5):695-704.
20. Haimovich B, Lipfert L, Brugge JS, Shattil SJ. Tyrosine phosphorylation and cytoskeletal reorganization in platelets are triggered by interaction of integrin receptors with their immobilized ligands. *J Biol Chem.* 1993;268(21):15868-15877.
21. Izaguirre G, Aguirre L, Ji P, Aneskievich B, Haimovich B. Tyrosine phosphorylation of alpha-actinin in activated platelets. *J Biol Chem.* 1999;274(52):37012-37020.
22. Izaguirre G, Aguirre L, Hu YP, et al. The cytoskeletal/non-muscle isoform of alpha-actinin is phosphorylated on its actin-binding domain by the focal adhesion kinase. *J Biol Chem.* 2001;276(31):28676-28685.
23. Lin SY, Raval S, Zhang Z, et al. The protein-tyrosine phosphatase SHP-1 regulates the phosphorylation of alpha-actinin. *J Biol Chem.* 2004; 279(24):25755-25764.
24. Shiraga M, Miyata S, Kato H, et al. Impaired platelet function in a patient with P2Y12 deficiency caused by a mutation in the translation initiation codon. *J Thromb Haemost.* 2005;3(10):2315-2323.
25. Tokuhira M, Handa M, Kamata T, et al. A novel regulatory epitope defined by a murine monoclonal antibody to the platelet GPIIb-IIIa complex (alphaIIbbeta3 integrin). *Thromb Haemost.* 1996; 76(6):1038-1046.
26. Honda S, Tomiyama Y, Aoki T, et al. Association between ligand-induced conformational changes of integrin alphaIIbbeta3 and alphaIIbbeta3-mediated intracellular Ca^{2+} signaling. *Blood.* 1998;92(10): 3675-3683.
27. Kashiwagi H, Shiraga M, Honda S, et al. Activation of integrin alphaIIbbeta3 in the glycoprotein Ib-high population of a megakaryocytic cell line, CMK, by inside-out signaling. *J Thromb Haemost.* 2004;2(1):177-186.
28. LaFlamme SE, Akiyama SK, Yamada KM. Regulation of fibronectin receptor distribution. *J Cell Biol.* 1992;117(2):437-447.
29. Kamae T, Shiraga M, Kashiwagi H, et al. Critical role of ADP interaction with P2Y12 receptor in the maintenance of alphaIIbbeta3 activation: association with Rap1B activation. *J Thromb Haemost.* 2006;4(6):1379-1387.
30. Shiraga M, Kamae T, Akiyama M, et al. P2Y12-independent transient activation and P2Y12-dependent prolonged activation of platelet integrin alphaIIbbeta3 [abstract]. *Blood.* 2006;108(11):435a. Abstract 1509.
31. Arabaci G, Guo XC, Beebe KD, Coggeshall KM, Pei D. alpha-Haloacetophenone derivatives as photoreversible covalent inhibitors of protein tyrosine phosphatases. *J Am Chem Soc.* 1999; 121(21):5085-5086.
32. Aleil B, Ravanat C, Cazenave JP, Rochoux G, Heitz A, Gachet C. Flow cytometric analysis of intraplatelet VASP phosphorylation for the detection of clopidogrel resistance in patients with ischemic cardiovascular diseases. *J Thromb Haemost.* 2005;3(1):85-92.
33. Kahn ML, Zheng YW, Huang W, et al. A dual thrombin receptor system for platelet activation. *Nature.* 1998;394(6694):690-694.
34. Covic L, Gresser AL, Kuliopulos A. Biphasic kinetics of activation and signaling for PAR1 and PAR4 thrombin receptors in platelets. *Biochemistry.* 2000;39(18):5458-5467.
35. Shapiro MJ, Weiss EJ, Faruqi TR, Coughlin SR. Protease activated receptor 1 and 4 are shut off with distinct kinetics after activation by thrombin. *J Biol Chem.* 2000;275(33):25216-25221.
36. Frojmovic M, Wong T, van de Ven T. Dynamic measurements of the platelet membrane glycoprotein IIb-IIIa receptor for fibrinogen by flow cytometry, I: methodology, theory and results for two distinct activators. *Biophys J.* 1991;59(4):815-827.
37. O'Toole TE, Loftus JC, Du XP, et al. Affinity modulation of the alphaIIbbeta3 integrin (platelet GPIIb-IIIa) is an intrinsic property of the receptor. *Cell Regul.* 1990;1(12):883-893.
38. Legate KR, Fässler R. Mechanisms that regulate adaptor binding to beta-integrin cytoplasmic tails. *J Cell Sci.* 2009;122(Pt 2):187-198.
39. Ye F, Hu G, Taylor D, et al. Recreation of the terminal events in physiological integrin activation. *J Cell Biol.* 2010;188(1):157-173.
40. Lau TL, Kim C, Ginsberg MH, Ulmer TS. The structure of the integrin alphaIIbbeta3 transmembrane complex explains integrin transmembrane signalling. *EMBO J.* 2009;28(9):1351-1361.
41. Lyman S, Gilmore A, Burridge K, Gidwitz S, White GCII. Integrin-mediated activation of focal adhesion kinase is independent of focal adhesion formation or integrin activation. Studies with activated and inhibitory beta3 cytoplasmic domain mutants. *J Biol Chem.* 1997;272(36):22538-22547.
42. von Wichert G, Haimovich B, Feng GS, Sheetz MP. Force-dependent integrin-cytoskeleton linkage formation requires downregulation of focal complex dynamics by Shp2. *EMBO J.* 2003;22(19):5023-5035.
43. Feng S, Lu X, Reséndiz JC, Kroll MH. Pathological shear stress directly regulates platelet alphaIIbbeta3 signaling. *Am J Physiol Cell Physiol.* 2006;291(6):C1346-C1354.
44. Tomiyama Y, Shiraga M, Kashiwagi H. Positive and negative regulation of integrin function. In: Tanaka K, Davie EW, eds. *Recent Advances in Thrombosis and Hemostasis 2008.* New York, NY: Springer;2008:243-252.
45. Brass LF, Zhu L, Stalker TJ. Minding the gaps to promote thrombus growth and stability. *J Clin Invest.* 2005;115(12):3385-3392.

Nuclear translocation of anamorsin during drug-induced dopaminergic neurodegeneration in culture and in rat brain

Journal of Neural Transmission
Basic Neurosciences, Genetics and Immunology, Movement disorders, Dementias, Biological Psychiatry, Biological Child and Adolescent Psychiatry

ISSN 0300-9564
Volume 118
Number 3

J Neural Transm (2011)
118:433-444
DOI 10.1007/
s00702-010-0490-8

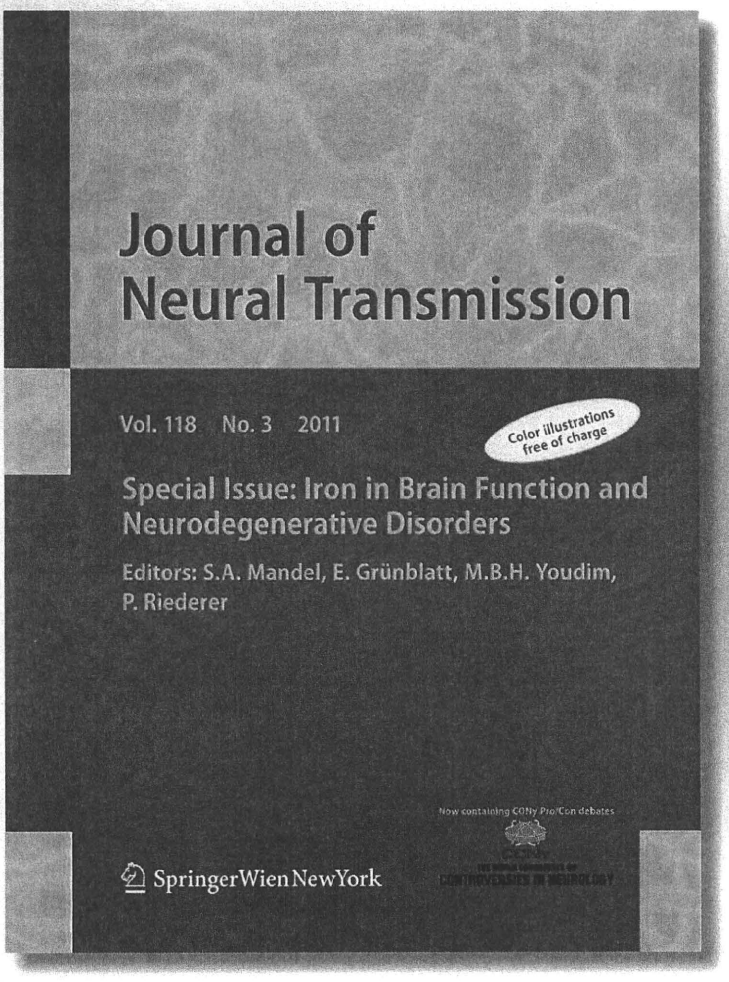

Springer

J Neural Transm (2011) 118:433–444
DOI 10.1007/s00702-010-0490-8

Nuclear translocation of anamorsin during drug-induced dopaminergic neurodegeneration in culture and in rat brain

Kyung-Ah Park · Nuri Yun · Dong-Ik Shin · So Yoen Choi · Hyun Kim · Won-Ki Kim · Yuzuru Kanakura · Hirohiko Shibayama · Young J. Oh

Received: 19 April 2010 / Accepted: 21 September 2010 / Published online: 6 October 2010

Abstract Anamorsin, also called cytokine-induced apoptosis inhibitor 1 (CIAPIN1), was recently identified to confer resistance to apoptosis induced by growth factor deprivation and to be indispensible for hematopoiesis. Recently, it was demonstrated that anamorsin is also widely distributed in both fetal and adult tissues. In this study, we evaluated the tissue distribution of anamorsin in the central nervous system (CNS) during development. In situ hybridization and immunoblot analyses revealed that anamorsin mRNA and protein were both highly and widely expressed in various regions of the CNS, including the cerebral cortex, hippocampus, midbrain, cerebellum, medulla, and spinal cord. Based on these findings, we examined its cellular localization during drug-induced neurodegeneration in MN9D dopaminergic cells. Both immunocytochemical localization and immunoblot analyses indicated that cytosolic anamorsin was translocated into the nucleus in a time-dependent manner following treatment with a reactive oxygen species (ROS)-inducing drug, 6-hydroxydopamine (6-OHDA). Treatment of cells with the apoptosis-inducing reagent, staurosporine, did not appear to cause translocation of anamorsin into the nucleus. When cells were treated with the nuclear export inhibitor, Leptomycin B, alone or with 6-OHDA, nuclear anamorsin levels increased, indicating that nuclear influx and efflux of anamorsin are regulated by 6-OHDA treatment. In rat brain injected with 6-OHDA, nuclear translocation of anamorsin was identified in certain tyrosine hydroxylase (TH)-positive neurons as well as TH-negative cells. Furthermore, treatment of MN9D cells with hydrogen peroxide or ROS-inducing trace metals caused nuclear translocation of anamorsin. Taken together, our data indicate that nuclear translocation of anamorsin is a ROS-dependent event and may participate in the regulation of transcription of critical molecules during dopaminergic neurodegeneration.

Keywords Anamorsin · 6-Hydroxydopamine · Trace metal elements · Reactive oxygen species · Nuclear translocation · Neurodegeneration

K.-A. Park · N. Yun · D.-I. Shin · Y. J. Oh (✉)
Department of Biology, Yonsei University College of Life Science and Biotechnology, 134 Shincheon-dong Seodaemoon-gu, Seoul 120-749, Korea
e-mail: yjoh@yonsei.ac.kr

S. Y. Choi · H. Kim · W.-K. Kim
Department of Anatomy and Brain Korea 21 Biomedical Science Program, Korea University College of Medicine, Seoul 136-705, Korea

Y. Kanakura · H. Shibayama
Department of Hematology and Oncology, Osaka University Graduate School of Medicine, Osaka 565-0871, Japan

Introduction

Parkinson's disease (PD) is a typical neurodegenerative disorder accompanied by the selective death of dopaminergic neurons in the substantia nigra pars compacta. Clinical symptoms include rigidity, resting tremor, and bradykinesia in patients with PD, which are caused by the loss of dopaminergic neurons and the subsequent depletion of dopamine in the striatum (Spillantini et al. 1997). Although the etiological cause of PD remains unclear, it has been proposed that dopaminergic neurodegeneration may result from the complicated interplay between genetic and environmental factors. Indeed, several critical mediators of PD have been proposed, based on both in vivo and in vitro pathophysiological models of PD established by treatment with dopaminergic neurotoxins, as well as

gene-based [e.g., α-synuclein, parkin, PINK1, LRRK2, and DJ-1 (Klein and Schlossmacher 2006; Moore et al. 2005)] experimental models that include oxidative stress, mitochondrial dysfunction, excitotoxicity, iron deposition, abnormal protein aggregation, and inflammation (Mattson 2000). With regard to cell death mechanisms involved in neurodegeneration, accumulating evidence indicates that oxidative stress is an emerging mediator that causes apoptosis, necrosis, and autophagy (Han et al. 2003a; Levine and Kroemer 2008; Mattson 2000; Rubinsztein et al. 2007). Despite the recent progress in our understanding of dopaminergic neurodegeneration, detailed molecular and cellular mechanisms remain to be further elucidated.

Currently, several approaches using proteomics have been reported to identify multiple target proteins and biomarkers critical for neurodegeneration (for reviews see Blennow et al. 2010; Licker et al. 2009; Pienaar et al. 2008). Both fluid and tissue samples obtained from pathophysiological and gene-based experimental models of PD or from patients with PD have been subjected to proteomics analyses (Basso et al. 2004; Jin et al. 2006; Van Laar et al. 2008; Zhang et al. 2008). To identify both the temporal and spatial protein expression patterns, we also utilized experimental models established by 6-hydroxydopamine (6-OHDA) treatment (Lee et al. 2003, 2008; Park et al. 2010). Neuroproteomics has many advantages over microarray analysis at the gene level to identify multiple protein–protein interactions, post-translational modifications, and cellular translocation. To explore disease-associated proteins that can be translocated during neurodegeneration, we conducted fractionation analyses of both cytosolic and nuclear fractions obtained from MN9D dopaminergic neuronal cells treated with or without 6-OHDA. Among many identified potential candidates, we found that anamorsin appeared to translocate from the cytosol to the nucleus following neurodegeneration. Anamorsin, also called cytokine-induced apoptosis inhibitor 1 (CIAPIN1), is known as an anti-apoptotic protein and was originally isolated as a molecule that conferred resistance to apoptosis induced by growth factor deprivation (Shibayama et al. 2004). Recently, it was demonstrated that anamorsin is widely distributed in almost all fetal and adult tissues, including brain (Hao et al. 2006). Similarly, its subcellular distribution and potential roles have been proposed (for review, Li et al. 2010). However, its distribution pattern and expression levels in the central nervous system (CNS) have not been thoroughly examined during development. The potential translocation of anamorsin into the nucleus has not been studied during drug-induced neurodegeneration. In the present study, therefore, we specifically investigated the distribution and expression of anamorsin in the brain and spinal cord during development as well as the nuclear translocation of anamorsin in both the midbrain following stereotaxic injection of 6-OHDA into the striatum and MN9D dopaminergic neuronal cells (Choi et al. 1991) treated with reactive oxygen species (ROS)-inducing drugs, such as 6-OHDA. Here, we found that anamorsin was widely distributed in various regions of the CNS during development. In dopaminergic neurodegeneration paradigms applied in the present study, anamorsin was translocated into the nucleus in the presence of ROS as evaluated by immunocytochemical, immunohistochemical, and immunoblot analyses.

Materials and methods

Probe construction and in situ hybridization

Polymerase chain reaction (PCR) fragments, encompassing nucleotides 409–909 (probe #1), 361–670 (probe #2), and 625–927 (probe #3), of mouse anamorsin (Genbank accession number AY523555) were subcloned into the p-GEM T easy vector (Promega). The PCR primer sequences were as follows: Probe #1: sense 5′-CCTGAGGAGGTACAGTCC GTGCA-3′ and antisense 5′-ATTGCTCAGGAGCACCTG CTCG-3′; Probe #2: sense 5′-CTTTCTGGCCTCGTGGA AATAAAAGA-3 and antisense 5′-CTCTTCAAATCCTC TGGATCAAGCAG-3′; and Probe #3: sense 5′-GATCT CATTGACTCAGACGAGCTGC-3′ and antisense 5′-CTA GGCATCCTGGAGATTGCTATTGCTC-3′. Two to three C57BL6 mice were assigned to each probe used for in situ hybridization. Brain of C57BL6 mouse was rapidly frozen in isopentane prechilled (−80°C), and the frozen brains were cut (12 μm-thick) and thaw-mounted onto (3-aminopropyl)triethoxy-saline (Sigma) coated slides and fixed in 4% paraformaldehyde. Sections were then treated with 0.25% acetic anhydride in 0.1 M triethanolamine/0.9% NaCl, pH 8.0, dehydrated and defatted in ethanol and chloroform, and finally air-dried. Riboprobe used in this study were directed against bases (probe #1:409–909, probe #2:361–670, and probe #3:625–927) of anamorsin. The antisense probes were in the presence of a-[^{35}S]UTP (Perkin Elmer) and sections were hybridized overnight at 63°C with labeled probe. On the next day, sections were washed in SSC, treated with 0.02 mg/ml RNase A (USB) in SSC for 30 min at 37°C and washed in the graded of serial SSC and dehydrated in ethanol. Hybridized sections were exposed to Biomax MR-1 (KODAK 8567232).

Cell culture and stable cell line construction

We used an MN9D dopaminergic neuronal cell line established by somatic fusion between embryonic mesencephalic neurons and N18TG cells (Choi et al. 1991). MN9D cells were transfected with a eukaryotic expression